

Solving Almost all Systems of Random Quadratic Equations

Gang Wang, Georgios B. Giannakis, Yousef Saad, and Jie Chen

Abstract

This paper deals with finding an n -dimensional solution \mathbf{x} to a system of quadratic equations of the form $y_i = |\langle \mathbf{a}_i, \mathbf{x} \rangle|^2$ for $1 \leq i \leq m$, which is also known as phase retrieval and is NP-hard in general. We put forth a novel procedure for minimizing the amplitude-based least-squares empirical loss, that starts with a weighted maximal correlation initialization obtainable with a few power or Lanczos iterations, followed by successive refinements based upon a sequence of iteratively reweighted (generalized) gradient iterations. The two (both the initialization and gradient flow) stages distinguish themselves from prior contributions by the inclusion of a fresh (re)weighting regularization technique. The overall algorithm is conceptually simple, numerically scalable, and easy-to-implement. For certain random measurement models, the novel procedure is shown capable of finding the true solution \mathbf{x} in time proportional to reading the data $\{(\mathbf{a}_i; y_i)\}_{1 \leq i \leq m}$. This holds with high probability and without extra assumption on the signal \mathbf{x} to be recovered, provided that the number m of equations is some constant $c > 0$ times the number n of unknowns in the signal vector, namely, $m > cn$. Empirically, the upshots of this contribution are: i) (almost) 100% perfect signal recovery in the high-dimensional (say e.g., $n \geq 2,000$) regime given only an *information-theoretic limit* number of noiseless equations, namely, $m = 2n - 1$ in the real-valued Gaussian case; and, ii) (nearly) optimal statistical accuracy in the presence of additive noise of bounded support. Finally, substantial numerical tests using both synthetic data and real images corroborate markedly improved signal recovery performance and computational efficiency of our novel procedure relative to state-of-the-art approaches.

Index terms— Nonconvex optimization, phase retrieval, iteratively reweighted gradient flow, convergence to global optimum, information-theoretic limit.

I. INTRODUCTION

One is often faced with solving quadratic equations of the form $y_i = |\langle \mathbf{a}_i, \mathbf{x} \rangle|^2$, or equivalently,

$$\psi_i = |\langle \mathbf{a}_i, \mathbf{x} \rangle|, \quad 1 \leq i \leq m \tag{1}$$

where $\mathbf{x} \in \mathbb{R}^n$ is the wanted unknown $n \times 1$ signal, while given observations ψ_i and feature/sensing vectors $\mathbf{a}_i \in \mathbb{R}^n$ that are collectively stacked in the data vector $\boldsymbol{\psi} := [\psi_i]_{1 \leq i \leq m}$ and the $m \times n$ sensing matrix $\mathbf{A} := [\mathbf{a}_i]_{1 \leq i \leq m}$, respectively. Put differently, given information about the (squared) modulus of the inner products of the signal vector \mathbf{x} and several known measurement vectors \mathbf{a}_i , can one reconstruct exactly (up to a global sign) \mathbf{x} , or alternatively, the missing signs of $\langle \mathbf{a}_i, \mathbf{x} \rangle$? In fact, much effort has recently been devoted to determining the number of such equations necessary and/or sufficient for the uniqueness of the solution \mathbf{x} ; see, for instance, [2], [3]. It has been proved that a number $m \geq 2n - 1$ of generic¹ (which includes the case of random vectors) measurement vectors \mathbf{a}_i are sufficient for uniquely

Work in this paper was supported partially by NSF grants 1500713 and 1514056. G. Wang and G. B. Giannakis are with the Digital Technology Center and the Department of Electrical and Computer Engineering, University of Minnesota, Minneapolis, MN 55455, USA. G. Wang is also with the State Key Lab of Intelligent Control and Decision of Complex Systems, Beijing Institute of Technology, Beijing 100081, P. R. China. Y. Saad is with the Department of Computer Science and Engineering, University of Minnesota, Minneapolis, MN 55455, USA. J. Chen is with the State Key Lab of Intelligent Control and Decision of Complex Systems, Beijing Institute of Technology, Beijing 100081, P. R. China. Emails: {gangwang, georgios, saad}@umn.edu; chenjie@bit.edu.cn.

¹It is out of the scope of the present paper to explain the meaning of generic vectors, whereas interested readers are referred to [2].

determining an n -dimensional real vector \mathbf{x} , while $m = 2n - 1$ is shown also necessary [2]. In this sense, the number $m = 2n - 1$ of equations as in (1) can be thought of as the information-theoretic limit for such a quadratic system to be solvable. Nevertheless, even for random measurement vectors, despite the existence of a unique solution given the minimal number $2n - 1$ of quadratic equations, it is unclear so far whether there is a numerical polynomial-time algorithm that is able to stably find the true solution (say e.g., with probability $\geq 99\%$)?

In diverse physical sciences and engineering fields, it is impossible or very difficult to record phase measurements. The problem of recovering the signal or phase from magnitude measurements only, also commonly known as phase retrieval, emerges naturally [19], [20], [29]. Relevant application domains include e.g., X-ray crystallography, ptychography, astronomy, and coherent diffraction imaging [29]. In such setups, optical measurement and detection systems record solely the photon flux, which is proportional to the (squared) magnitude of the field, but not the phase. Problem (1) in its squared form, on the other hand, can be readily recast as an instance of nonconvex quadratically constrained quadratic programming (QCQP), that subsumes as special cases several well-known combinatorial optimization problems involving Boolean variables, e.g., the NP-complete stone problem [4, Sec. 3.4.1]. A related task of this kind is that of estimating the mixture of linear regressions, where the latent membership indicators can be converted into the missing phases [38]. Although of simple form and practical relevance across different fields, solving systems of nonlinear equations is arguably the most difficult problem in all of the numerical computations [27, Page 355].

Regarding common notation used throughout this paper, lower- (upper-) case boldface letters denote vectors (matrices). Calligraphic letters are reserved for sets, e.g., \mathcal{S} . Symbol A/B means either A or B , while fractions are denoted by A/B . The floor operation $\lfloor c \rfloor$ gives the largest integer no greater than the given number $c > 0$, $|\mathcal{S}|$ the number of entries in set \mathcal{S} , and $\|\mathbf{x}\|$ is the Euclidean norm. Since $\mathbf{x} \in \mathbb{R}^n$ and $-\mathbf{x}$ are indistinguishable given $\{\psi_i\}$, let $\text{dist}(\mathbf{z}, \mathbf{x}) = \min\{\|\mathbf{z} + \mathbf{x}\|, \|\mathbf{z} - \mathbf{x}\|\}$ be the Euclidean distance of any estimate $\mathbf{z} \in \mathbb{R}^n$ to the solution set $\{\pm \mathbf{x}\}$ of (1).

A. Prior contributions

Following the least-squares criterion (which coincides with the maximum likelihood one assuming additive white Gaussian noise), the problem of solving systems of quadratic equations can be naturally recast as the ensuing empirical loss minimization

$$\underset{\mathbf{z} \in \mathbb{R}^n}{\text{minimize}} \quad L(\mathbf{z}) := \frac{1}{m} \sum_{i=1}^m \ell(\mathbf{z}; \psi_i / y_i) \quad (2)$$

where one can choose to work with the *amplitude-based* loss function $\ell(\mathbf{z}; \psi_i) := (\psi_i - |\langle \mathbf{a}_i, \mathbf{z} \rangle|)^2 / 2$ [36], or the *intensity-based* ones $\ell(\mathbf{z}; y_i) := (y_i - |\langle \mathbf{a}_i, \mathbf{z} \rangle|^2)^2 / 2$ [7], [18], and its related Poisson likelihood $\ell(\mathbf{z}; y_i) := y_i \log(|\langle \mathbf{a}_i, \mathbf{z} \rangle|^2) - |\langle \mathbf{a}_i, \mathbf{z} \rangle|^2$ [14]. Either way, the objective functional $L(\mathbf{z})$ is rendered nonconvex; hence, it is in general NP-hard and computationally intractable to compute the least-squares or the maximum likelihood estimate (MLE) [4].

Minimizing the squared modulus-based least-squares loss in (2), several numerical polynomial-time algorithms have been devised based on convex programming for certain choices of design vectors \mathbf{a}_i [9], [8], [33], [13], [6], [24]. Relying upon the so-called matrix-lifting technique (a.k.a, Shor's relaxation), semidefinite programming (SDP) based convex approaches first express all intensity data into linear terms in a new rank-1 matrix variable, followed by solving a convex SDP after dropping the rank constraint (a.k.a., semidefinite relaxation). It has been established that perfect recovery and (near-)optimal statistical accuracy can be achieved in noiseless and noisy settings respectively with an optimal-order number of

measurements [6]. In terms of computational efficiency however, convex approaches entail storing and solving for an $n \times n$ semi-definite matrix, whose worst-case computational complexity scales as $n^{4.5} \log 1/\epsilon$ provided that the number m of constraints is on the order of the dimension n [33], which does not scale well to high-dimensional tasks. Another recent line of convex relaxation [21], [1], [22] reformulated the problem of phase retrieval as that of sparse signal recovery, and solves a linear program in the natural parameter vector domain. Although exact signal recovery can be established assuming an accurate enough anchor vector, its empirical performance is not competitive with state-of-the-art phase retrieval approaches.

Instead of convex relaxation, recent proposals also advocate judiciously initialized iterative procedures for coping with certain nonconvex formulations directly, which include solvers based on e.g., alternating minimization [26], Wirtinger flow [7], [14], [40], [39], [5], [30], [11], amplitude flow [36], [35], [37], [34], as well as a prox-linear procedure via composite optimization [16], [17]. These nonconvex approaches operate directly upon vector optimization variables, therefore leading to significant computational advantages over matrix-lifting based convex counterparts. With random features, they can be interpreted as performing stochastic optimization over acquired data samples $\{(\mathbf{a}_i; \psi_i/y_i)\}_{1 \leq i \leq m}$ to approximately minimize the population risk functional $\bar{L}(\mathbf{z}) := \mathbb{E}_{(\mathbf{a}_i, \psi_i/y_i)}[\ell(\mathbf{z}; \psi_i/y_i)]$. It is well documented that minimizing nonconvex functionals is computationally intractable in general due to existence of multiple stationary points [4]. Assuming random Gaussian sensing vectors however, such nonconvex paradigms can provably locate the global optimum under suitable conditions, some of which also achieve optimal (statistical) guarantees. Specifically, starting with a judiciously designed initial guess, successive improvement is effected based upon a sequence of (truncated) (generalized) gradient iterations given by

$$\mathbf{z}^{t+1} := \mathbf{z}^t - \frac{\mu^t}{m} \sum_{i \in \mathcal{T}^{t+1}} \nabla \ell_i(\mathbf{z}^t; \psi_i/y_i), \quad t = 0, 1, \dots \quad (3)$$

where \mathbf{z}^t denotes the estimate returned by the algorithm at the t -th iteration, $\mu^t > 0$ the learning rate, and $\nabla \ell(\mathbf{z}^t, \psi_i/y_i)$ is the (generalized) gradient of the modulus- or squared modulus-based least-squares loss evaluated at \mathbf{z}^t [15]. Here, \mathcal{T}^{t+1} represents some time-varying index set signifying and effecting the per-iteration truncation.

Although they achieve optimal statistical guarantees in both noiseless and noisy settings, state-of-the-art (convex and nonconvex) approaches studied under random Gaussian designs, empirically require stable recovery of a number of equations (several) times larger than the aforementioned information-theoretic limit [14], [7], [40]. As a matter of fact, when there are numerous enough measurements (on the order of the signal dimension n up to some polylog factors), the modulus-square based least-squares loss functional admits benign geometric structure in the sense that [31]: with high probability, i) all local minimizers are global; and, ii) there always exists a negative directional curvature at every saddle point. In a nutshell, the grand challenge of solving systems of random quadratic equations remains to develop numerical polynomial-time algorithms capable of achieving perfect recovery and optimal statistical accuracy when the number of measurements approaches the information-theoretic limit.

B. This work

Building upon but going beyond the scope of the aforementioned nonconvex paradigms, the present paper puts forward a novel iterative linear-time procedure, namely, time proportional to that required by the processor to scan the entire data $\{(\mathbf{a}_i; \psi_i)\}_{1 \leq i \leq m}$, which we term *reweighted amplitude flow* and abbreviate as RAF. Our methodology is capable of solving noiseless random quadratic equations exactly, and of constructing an estimate of (near)-optimal statistical accuracy from noisy modulus observations. Exactness and accuracy hold with high probability and without extra assumption on the signal \mathbf{x} to be recovered,

provided that the ratio m/n of the number of measurements to that of the unknowns exceeds some large constant. Empirically, our approach is demonstrated to be able to achieve perfect recovery of arbitrary high-dimensional signals given a *minimal* number of equations, which in the real case is $m = 2n - 1$. The new twist here is to leverage judiciously designed yet conceptually simple (iterative)(re)weighting regularization techniques to enhance existing initializations and also gradient refinements. An informal depiction of our RAF methodology is given in two stages below, with rigorous algorithmic details deferred to Section III:

- S1) Weighted maximal correlation initialization:** Obtain an initializer \mathbf{z}^0 maximally correlated with a carefully selected subset $\mathcal{S} \subsetneq \mathcal{M} := \{1, 2, \dots, m\}$ of feature vectors \mathbf{a}_i , whose contributions toward constructing \mathbf{z}^0 are judiciously weighted by suitable parameters $\{w_i^0 > 0\}_{i \in \mathcal{S}}$.

- S2) Iteratively reweighted “gradient-like” iterations:** Loop over $0 \leq t \leq T$

$$\mathbf{z}^{t+1} = \mathbf{z}^t - \frac{\mu^t}{m} \sum_{i=1}^m w_i^t \nabla \ell(\mathbf{z}^t; \psi_i) \quad (4)$$

for some time-varying weights $w_i^t \geq 0$ that are adaptive in time, each depending on the current iterate \mathbf{z}_t and the datum $(\mathbf{a}_i; \psi_i)$.

Two attributes of our novel methodology are worth highlighting. First, albeit being a variant of the orthogonality-promoting initialization [36], the initialization here [cf. S1)] is distinct in the sense that different importance is attached to each selected datum $(\mathbf{a}_i; \psi_i)$, or more precisely, to each selected directional vector \mathbf{a}_i . Likewise, the gradient flow [cf. S2)] weights judiciously the search direction suggested by each datum $(\mathbf{a}_i; \psi_i)$. In this manner, more accurate and robust initializations as well as more stable overall search directions in the gradient flow stage can be obtained even based only on a relatively limited number of data samples. Moreover, with particular choices of weights w_i^t 's (for example, when they take 0/1 values), our methodology subsumes as special cases the recently proposed truncated amplitude flow (TAF) [36] and reshaped Wirtinger flow (RWF) [40].

The reminder of this paper is structured as follows. The two stages of our RAF algorithm are motivated and developed in Section II, and Section III summarizes the algorithm and establishes its theoretical performance. Extensive numerical tests evaluating the performance of RAF relative to state-of-the-art approaches are presented in Section IV, while useful technical lemmas and main proof ideas are given in Section V. Concluding remarks are drawn in VI, and technical proof details are provided in the Appendix at the end of the paper.

II. ALGORITHM: REWEIGHTED AMPLITUDE FLOW

This section explains the intuition and the basic principles behind each stage of RAF in detail. For theoretical concreteness, we focus on the *real-valued Gaussian model* with a real signal \mathbf{x} , and independent Gaussian random measurement vectors $\mathbf{a}_i \sim \mathcal{N}(\mathbf{0}, \mathbf{I})$, $1 \leq i \leq m$. Nevertheless, our RAF approach can be applied without algorithmic changes even when the complex-valued Gaussian with $\mathbf{x} \in \mathbb{C}^n$ and independent $\mathbf{a}_i \sim \mathcal{CN}(\mathbf{0}, \mathbf{I}_n) := \mathcal{N}(\mathbf{0}, \mathbf{I}_n/2) + j\mathcal{N}(\mathbf{0}, \mathbf{I}_n/2)$, and also the coded diffraction pattern (CDP) models are considered.

A. Weighted maximal correlation initialization

A key enabler of general nonconvex iterative heuristics' success in finding the global optimum is to seed them with an excellent starting point [23]. In fact, several smart initialization strategies have been advocated for iterative phase retrieval algorithms; see e.g., the spectral [26], [7], truncated spectral [14], [40], and orthogonality-promoting [36] initializations. One promising approach among them is the one

proposed in [36], which is robust to outliers [16], and also enjoys better phase transitions than the spectral procedures [25]. To hopefully achieve perfect signal recovery at the information-theoretic limit however, its numerical performance may still need further enhancement. On the other hand, it is intuitive that to improve the initialization performance (over state-of-the-art schemes) becomes increasingly challenging as the number of acquired data samples approaches the information-theoretic limit of $m = 2n - 1$.

In this context, we develop a more flexible initialization scheme based on the correlation property (as opposed to the orthogonality), in which the added benefit relative to the initialization procedure in [36] is the inclusion of a flexible weighting regularization technique to better balance the useful information exploited in all selected data. In words, we introduce judiciously designed weights to the initialization procedure developed in [36]. Similar to related approaches, our strategy entails estimating both the norm $\|\boldsymbol{x}\|$ and the unit direction $\boldsymbol{x}/\|\boldsymbol{x}\|$. Leveraging the strong law of large numbers and the rotational invariance of Gaussian \boldsymbol{a}_i sampling vectors (the latter suffices to assume $\boldsymbol{x} = \|\boldsymbol{x}\|\boldsymbol{e}_1$, with \boldsymbol{e}_1 being the first canonical vector in \mathbb{R}^n), it is clear that

$$\frac{1}{m} \sum_{i=1}^m \psi_i^2 = \frac{1}{m} \sum_{i=1}^m |\langle \boldsymbol{a}_i, \|\boldsymbol{x}\|\boldsymbol{e}_1 \rangle|^2 = \left(\frac{1}{m} \sum_{i=1}^m a_{i,1}^2 \right) \|\boldsymbol{x}\|^2 \approx \|\boldsymbol{x}\|^2 \quad (5)$$

whereby $\|\boldsymbol{x}\|$ can be estimated to be $\sum_{i=1}^m \psi_i^2/m$. This estimate proves very accurate even with an information-theoretic limit number of data samples because it is unbiased and tightly concentrated.

The challenge thus lies in accurately estimating the direction of \boldsymbol{x} , or seeking a unit vector maximally aligned with \boldsymbol{x} , which is a bit tricky. To gain intuition into our initialization strategy, let us first present a variant of the initialization in [36], whose robust counterpart to outlying measurements has been recently discussed in [16]. Note that the larger the modulus ψ_i of the inner-product between \boldsymbol{a}_i and \boldsymbol{x} is, the known design vector \boldsymbol{a}_i is deemed *more correlated* to the unknown solution \boldsymbol{x} , hence bearing useful directional information of \boldsymbol{x} . Inspired by this fact and based on available data $\{(\boldsymbol{a}_i; \psi_i)\}_{1 \leq i \leq m}$, one can sort all (absolute) correlation coefficients $\{\psi_i\}_{1 \leq i \leq m}$ in an ascending order, to yield ordered coefficients denoted by $0 < \psi_{[m]} \leq \dots \leq \psi_{[2]} \leq \psi_{[1]}$. Sorting m records takes time proportional to $\mathcal{O}(m \log m)$.² Let $\mathcal{S} \subsetneq \mathcal{M}$ represent the set of selected feature vectors \boldsymbol{a}_i to be used for computing the initialization, which is to be designed next. Fix *a priori* the cardinality $|\mathcal{S}|$ to some integer on the order of m , say, $|\mathcal{S}| := \lfloor 3m/13 \rfloor$. It is then natural to *define* \mathcal{S} to collect the \boldsymbol{a}_i vectors that correspond to one of the largest $|\mathcal{S}|$ correlation coefficients $\{\psi_{[i]}\}_{1 \leq i \leq |\mathcal{S}|}$, each of which can be thought of as pointing to (roughly) the direction of \boldsymbol{x} . Approximating the direction of \boldsymbol{x} thus boils down to finding a vector to maximize its correlation with the subset \mathcal{S} of selected directional vectors \boldsymbol{a}_i . Succinctly, the wanted approximation vector can be efficiently found as the solution of

$$\underset{\|\boldsymbol{z}\|=1}{\text{maximize}} \frac{1}{|\mathcal{S}|} \sum_{i \in \mathcal{S}} |\langle \boldsymbol{a}_i, \boldsymbol{z} \rangle|^2 = \boldsymbol{z}^* \left(\frac{1}{|\mathcal{S}|} \sum_{i \in \mathcal{S}} \boldsymbol{a}_i \boldsymbol{a}_i^* \right) \boldsymbol{z} \quad (6)$$

where the superscript * represents the transpose. Upon scaling the solution of (6) by the norm estimate $\sum_{i=1}^m \psi_i^2/m$ in (5) to match the size of \boldsymbol{x} , we obtain what we will henceforth refer to as maximal correlation initialization.

As long as $|\mathcal{S}|$ is chosen on the order of m , the maximal correlation method outperforms the spectral ones in [7], [26], [14], and has comparable performance to the orthogonality-promoting method [36]. Its empirical performance around the information-theoretic limit however, is still not the best that we can hope for. Observe that all directional vectors $\{\boldsymbol{a}_i\}_{i \in \mathcal{S}}$ selected for forming the matrix $\bar{\mathbf{Y}} := \frac{1}{|\mathcal{S}|} \sum_{i \in \mathcal{S}} \boldsymbol{a}_i \boldsymbol{a}_i^*$ in (6) are treated *the same* in terms of their contributions to constructing the (direction of the) initialization.

² $f(m) = \mathcal{O}(g(m))$ means that there exists a constant $C > 0$ such that $|f(m)| \leq C|g(m)|$.

Nevertheless, according to our starting principle, this ordering information carried by the selected \mathbf{a}_i vectors has *not* been exploited by the initialization scheme in (6) (see also [36], [16]). In words, if for selected data $i, j \in \mathcal{S}$, the correlation coefficient of ψ_i with \mathbf{a}_i is larger than that of ψ_j with \mathbf{a}_j , then \mathbf{a}_i is deemed more correlated (with \mathbf{x}) than \mathbf{a}_j is, hence bearing more useful information about the wanted direction of \mathbf{x} . It is thus prudent to weight more (i.e., attach more importance to) the selected \mathbf{a}_i vectors corresponding to larger ψ_i values. Given the ordering information $\psi_{[|\mathcal{S}|]} \leq \dots \leq \psi_{[2]} \leq \psi_{[1]}$ available from the sorting procedure, a natural way to achieve this goal is weighting each \mathbf{a}_i vector with simple functions of ψ_i , say e.g., taking the weights $w_i^0 := \psi_i^\gamma$, $\forall i \in \mathcal{S}$, with the exponent parameter $\gamma \geq 0$ chosen to maintain the wanted ordering $w_{|\mathcal{S}|}^0 \leq \dots \leq w_{[2]}^0 \leq w_{[1]}^0$. In a nutshell, a more flexible initialization scheme, that we refer to as *weighted maximal correlation*, can be summarized as follows

$$\tilde{\mathbf{z}}_0 := \arg \max_{\|\mathbf{z}\|=1} \mathbf{z}^* \left(\frac{1}{|\mathcal{S}|} \sum_{i \in \mathcal{S}} \psi_i^\gamma \mathbf{a}_i \mathbf{a}_i^* \right) \mathbf{z} \quad (7)$$

which can be efficiently evaluated in time proportional to $\mathcal{O}(n|\mathcal{S}|)$ by means of the power method or the Lanczos algorithm [28]. The proposed initialization can be obtained upon scaling $\tilde{\mathbf{z}}_0$ from (7) by the norm estimate, to yield $\mathbf{z}_0 := (\sum_{i=1}^m \psi_i^2 / m)^{-1/2} \tilde{\mathbf{z}}_0$. By default, we take $\gamma := 1/2$ in all reported numerical implementations, yielding weights $w_i^0 := \sqrt{|\langle \mathbf{a}_i, \mathbf{x} \rangle|}$ for all $i \in \mathcal{S}$.

Regarding the initialization procedure in (7), we next highlight two features, while details and theoretical performance guarantees are provided in Section III:

- F1)** The weights $\{w_i^0\}$ in the maximal correlation scheme enable leveraging useful information that each feature vector \mathbf{a}_i may bear regarding the direction of \mathbf{x} .
- F2)** Taking $w_i^0 := \psi_i^\gamma$ for all $i \in \mathcal{S}$ and 0 otherwise, problem (7) can be equivalently rewritten as

$$\tilde{\mathbf{z}}_0 := \arg \max_{\|\mathbf{z}\|=1} \mathbf{z}^* \left(\frac{1}{m} \sum_{i=1}^m w_i^0 \mathbf{a}_i \mathbf{a}_i^* \right) \mathbf{z} \quad (8)$$

which subsumes existing initialization schemes with particular selections of weights. For instance, the “plain-vanilla” spectral initialization in [26], [7] is recovered by choosing $\mathcal{S} := \mathcal{M}$, and $w_i^0 := \psi_i^2$ for all $1 \leq i \leq m$.

For numerical comparison, define the Relative error := $\text{dist}(\mathbf{z}, \mathbf{x}) / \|\mathbf{x}\|$. All simulated results reported in this paper were averaged over 100 Monte Carlo (MC) realizations. Figure 1 evaluates the performance of the proposed initialization relative to several state-of-the-art strategies, and also with the information limit number of data benchmarking the minimal number of samples required. It is clear that our initialization is: i) consistently better than the state-of-the-art; and, ii) stable as the signal dimension n grows, which is in sharp contrast to the instability encountered by the spectral ones [26], [7], [14], [40]. It is also worth stressing that the about 5% empirical advantage (over the best [36]) at the challenging *information-theoretic benchmark* is indeed nontrivial, and is one of the main RAF upshots. This numerical advantage becomes increasingly pronounced as the ratio m/n of the number of equations to the unknowns grows. In this regard, our proposed initialization procedure may be combined with other iterative phase retrieval approaches to improve their numerical performance.

B. Adaptively reweighted gradient flow

For independent data adhering to the real-valued Gaussian model, the direction that TAF moves along in stage S2) presented earlier is given by the following (generalized) gradient [36], [15]:

$$\frac{1}{m} \sum_{i \in \mathcal{T}} \nabla \ell(\mathbf{z}; \psi_i) = \frac{1}{m} \sum_{i \in \mathcal{T}} \left(\mathbf{a}_i^* \mathbf{z} - \psi_i \frac{\mathbf{a}_i^* \mathbf{z}}{|\mathbf{a}_i^* \mathbf{z}|} \right) \mathbf{a}_i \quad (9)$$

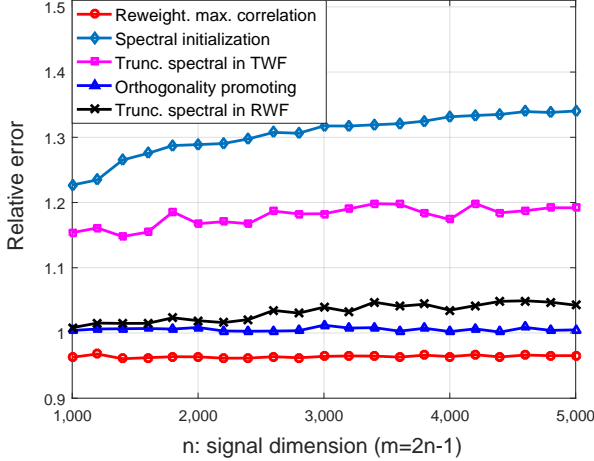


Fig. 1. Relative initialization error for the real-valued Gaussian model with $n = 1,000$ and $m = 2n - 1 = 1,999$.

where the dependence on the iterate count t is neglected for notational brevity, and the convention $a_i^* z / |a_i^* z| := 0$ is adopted if $a_i^* z = 0$.

Unfortunately, the (negative) gradient of the average in (9) may not point towards the true \boldsymbol{x} unless the current iterate \boldsymbol{z} is already very close to \boldsymbol{x} . As a consequence, moving along such a descent direction may not drag \boldsymbol{z} closer to \boldsymbol{x} . To see this, consider an initial guess \boldsymbol{z}_0 that has already been in a *basin of attraction* (i.e., a region within which there is only a unique stationary point) of \boldsymbol{x} . Certainly, there are summands $(a_i^* \boldsymbol{z} - \psi_i a_i^* \boldsymbol{z} / |a_i^* \boldsymbol{z}|) a_i$ in (9), that could give rise to “bad/misleading” search directions due to the erroneously estimated signs $a_i^* \boldsymbol{z} / |a_i^* \boldsymbol{z}| \neq a_i^* \boldsymbol{x} / |a_i^* \boldsymbol{x}|$ in (9) [36]. Those gradients as a whole may drag \boldsymbol{z} away from \boldsymbol{x} , and hence out of the basin of attraction. Such an effect becomes increasingly severe as the number m of acquired examples approaches the information-theoretic limit of $2n - 1$, thus rendering past approaches less effective in this case. Although this issue is somewhat remedied by TAF with a truncation procedure, its efficacy is still limited due to misses of bad gradients and mis-rejections of meaningful ones around the information-theoretic limit.

To address this challenge, our reweighted gradient flow effecting suitable search directions from *almost all* acquired data samples $\{(a_i; \psi_i)\}_{1 \leq i \leq m}$ will be adopted in a (timely) adaptive fashion; that is,

$$\boldsymbol{z}^{t+1} = \boldsymbol{z}^t - \mu^t \nabla \ell_{\text{rw}}(\boldsymbol{z}^t; \psi_i), \quad t = 0, 1, \dots \quad (10)$$

The *reweighted gradient* $\nabla \ell_{\text{rw}}(\boldsymbol{z}^t)$ evaluated at the current point \boldsymbol{z}^t is given as

$$\nabla \ell_{\text{rw}}(\boldsymbol{z}) := \frac{1}{m} \sum_{i=1}^m w_i \nabla \ell(\boldsymbol{z}; \psi_i) \quad (11)$$

for suitable weights $\{w_i\}_{1 \leq i \leq m}$ to be designed shortly.

To that end, we observe that the truncation criterion $\mathcal{T} := \{1 \leq i \leq m : |a_i^* \boldsymbol{z}| / |a_i^* \boldsymbol{x}| \geq \alpha\}$ with some given parameter $\alpha > 0$ suggests to include only gradients associated with $|a_i^* \boldsymbol{z}|$ of relatively large sizes. This is because gradients of sizable $|a_i^* \boldsymbol{z}| / |a_i^* \boldsymbol{x}|$ offer reliable and meaningful directions pointing to the truth \boldsymbol{x} with large probability [36]. As such, the ratio $|a_i^* \boldsymbol{z}| / |a_i^* \boldsymbol{x}|$ can be somewhat viewed as a confidence score about the reliability or meaningfulness of the corresponding gradient $\nabla \ell(\boldsymbol{z}; \psi_i)$. Recognizing that confidence can vary, it is natural to distinguish the contributions that different gradients make to the overall

search direction. An easy way is to attach large weights to the reliable gradients, and small weights to the spurious ones. Assume without loss of generality that $0 \leq w_i \leq 1$ for all $1 \leq i \leq m$; otherwise, lump the normalization factor achieving this into the learning rate μ^t . Building upon this observation and leveraging the gradient reliability confidence score $|\alpha_i^* z|/|\alpha_i^* x|$, the weight per gradient $\nabla \ell(z; \psi_i)$ in our proposed RAF algorithm is designed to be

$$w_i := \frac{1}{1 + \beta_i / (|\alpha_i^* z|/|\alpha_i^* x|)}, \quad 1 \leq i \leq m \quad (12)$$

where $\{\beta_i > 0\}_{1 \leq i \leq m}$ are some pre-selected parameters.

Regarding the weighting criterion in (29), three remarks are in order:

- R1)** The weights $\{w_i^t\}_{1 \leq i \leq m}$ are time adapted to the iterate z^t . One can also interpret the reweighted gradient flow z^{t+1} in (10) as performing a single gradient step to minimize the *smooth reweighted* loss $\frac{1}{m} \sum_{i=1}^m w_i^t \ell(z; \psi_i)$ with starting point z^t ; see also [10] for related ideas successfully exploited in the *iteratively reweighted least-squares* approach to compressive sampling.
- R2)** Note that the larger the confidence score $|\alpha_i^* z|/|\alpha_i^* x|$ is, the larger the corresponding weight w_i will be. More importance will be then attached to reliable gradients than to spurious ones. Gradients from *almost all* data are accounted for, which is in contrast to [36], where withdrawn gradients do not contribute the information they carry.
- R3)** At the points $\{z\}$ where $\alpha_i^* z = 0$ for some datum $i \in \mathcal{M}$, the i -th weight will be $w_i = 0$. In other words, the squared losses $\ell(z; \psi_i)$ in (2) that are nonsmooth at points z will be eliminated, to prevent their contribution to the reweighted gradient update in (10). Hence, the convergence analysis of RAF is considerably simplified because it does not have to cope with the nonsmoothness of the objective function in (2).

Having elaborated on the two stages, RAF can be readily summarized in Algorithm 1.

C. Algorithmic parameters

To optimize the empirical performance and facilitate numerical implementations, choice of pertinent algorithmic parameters of RAF is independently discussed here. It is obvious that the RAF algorithm entails four parameters. Our theory and all experiments are based on: i) $|\mathcal{S}|/m \leq 0.25$; ii) $0 \leq \beta_i \leq 10$ for all $1 \leq i \leq m$; and, iii) $0 \leq \gamma \leq 1$. For convenience, a constant step size $\mu^t \equiv \mu > 0$ is suggested, but other step size rules such as backtracking line search with the reweighted objective work as well. As will be formalized in Section III, RAF converges if the constant μ is not too large, with the upper bound depending in part on the selection of $\{\beta_i\}_{1 \leq i \leq m}$.

In the numerical tests presented in Section II and IV, we take $|\mathcal{S}| := \lfloor 3m/13 \rfloor$, $\beta_i \equiv \beta := 10$, $\gamma := 0.5$, and $\mu := 2$ (larger step sizes can be afforded for larger m/n values).

III. MAIN RESULTS

Our main result summarized in Theorem 1 next establishes exact recovery under the real-valued Gaussian model, whose proof is postponed to Section V for readability. Our RAF methodology however can be generalized readily to the complex Gaussian and CDP models.

Theorem 1 (Exact recovery). *Consider m noiseless measurements $\psi = |\mathbf{A}x|$ for an arbitrary signal $x \in \mathbb{R}^n$. If $m \geq c_0 |\mathcal{S}| \geq c_1 n$ with $|\mathcal{S}|$ being the pre-selected subset cardinality in the initialization step and the learning rate $\mu \leq \mu_0$, then with probability at least $1 - c_3 e^{-c_2 m}$, the reweighted amplitude flow's estimates z^t in Algorithm 1 obey*

$$\text{dist}(z^t, x) \leq \frac{1}{10} (1 - \nu)^t \|x\|, \quad t = 0, 1, \dots \quad (15)$$

Algorithm 1 Reweighted Amplitude Flow

- 1: **Input:** Data $\{(\mathbf{a}_i; \psi_i)\}_{1 \leq i \leq m}$; maximum number of iterations T ; step sizes $\mu^t = 2/6$ and weighting parameters $\beta_i = 10/5$ for real-/complex-valued Gaussian models; subset cardinality $|\mathcal{S}| = \lfloor 3m/13 \rfloor$, and exponent $\gamma = 0.5$.
- 2: **Construct** \mathcal{S} to include indices associated with the $|\mathcal{S}|$ largest entries among $\{\psi_i\}_{1 \leq i \leq m}$.
- 3: **Initialize** $\mathbf{z}^0 := \sqrt{\sum_{i=1}^m \psi_i^2/m} \tilde{\mathbf{z}}^0$ with $\tilde{\mathbf{z}}^0$ being the unit principal eigenvector of

$$\mathbf{Y} := \frac{1}{m} \sum_{i=1}^m w_i^0 \mathbf{a}_i \mathbf{a}_i^*, \quad \text{where } w_i^0 := \begin{cases} \psi_i^\gamma, & i \in \mathcal{S} \subseteq \mathcal{M} \\ 0, & \text{otherwise} \end{cases}. \quad (13)$$

- 4: **Loop:** **for** $t = 0$ **to** $T - 1$

$$\mathbf{z}^{t+1} = \mathbf{z}^t - \frac{\mu^t}{m} \sum_{i=1}^m w_i^t \left(\mathbf{a}_i^* \mathbf{z}^t - \psi_i \frac{\mathbf{a}_i^* \mathbf{z}^t}{|\mathbf{a}_i^* \mathbf{z}^t|} \right) \mathbf{a}_i \quad (14)$$

where $w_i^t := \frac{|\mathbf{a}_i^* \mathbf{z}^t|/\psi_i}{|\mathbf{a}_i^* \mathbf{z}^t|/\psi_i + \beta_i}$ for all $1 \leq i \leq m$.

- 5: **Output:** \mathbf{z}^T .
-

where $c_0, c_1, c_2, c_3 > 0$, $0 < \nu < 1$, and $\mu_0 > 0$ are certain numerical constants depending on the choice of algorithmic parameters $|\mathcal{S}|$, β , γ , and μ .

According to Theorem 1, a few interesting properties of our RAF algorithm are worth highlighting. To start, RAF recovers the true solution exactly with high probability whenever the ratio m/n of the number of equations to the unknowns exceeds some numerical constant. Expressed differently, RAF achieves the information-theoretic optimal order of sample complexity, which is consistent with the state-of-the-art including truncated Wirtinger flow (TWF) [14], TAF [36], and RWF [40]. Notice that the error contraction in (15) also holds at $t = 0$, namely, $\text{dist}(\mathbf{z}^0, \mathbf{x}) \leq \|\mathbf{x}\|/10$, therefore providing theoretical performance guarantees for the proposed initialization strategy (cf. Step 3 of Algorithm 1). Moreover, starting from this initial estimate, RAF converges exponentially fast to the true solution \mathbf{x} . In other words, to reach any ϵ -relative solution accuracy (i.e., $\text{dist}(\mathbf{z}^T, \mathbf{x}) \leq \epsilon \|\mathbf{x}\|$), it suffices to run at most $T = \mathcal{O}(\log 1/\epsilon)$ RAF iterations in Step 4 of Algorithm 1. This in conjunction with the per-iteration complexity $\mathcal{O}(mn)$ (namely, the complexity of one reweighted gradient update in (76)) confirms that RAF solves exactly a quadratic system in time $\mathcal{O}(mn \log 1/\epsilon)$, which is linear in $\mathcal{O}(mn)$, the time required by the processor to read the entire data $\{(\mathbf{a}_i; \psi_i)\}_{1 \leq i \leq m}$. Given the fact that the initialization stage can be performed in time $\mathcal{O}(n|\mathcal{S}|)$ and $|\mathcal{S}| < m$, the overall linear-time complexity of RAF is order-optimal.

IV. SIMULATED TESTS

Our theoretical findings about RAF have been corroborated with comprehensive numerical experiments, a sample of which are discussed next. Performance of RAF is evaluated relative to the state-of-the-art (T)WF [7], [14], RWF [40], and TAF [36] in terms of the empirical success rate among 100 MC realizations, where a success will be declared for an independent trial if the returned estimate incurs error $\|\psi - \mathbf{A}\mathbf{z}^T\|/\|\mathbf{x}\|$ less than 10^{-5} . Both the real Gaussian and the physically realizable CDP models were simulated. For fairness, all procedures were implemented with their suggested parameter values. We generated the truth $\mathbf{x} \sim \mathcal{N}(\mathbf{0}, \mathbf{I})$, and i.i.d. measurement vectors $\mathbf{a}_i \sim \mathcal{N}(\mathbf{0}, \mathbf{I})$, $1 \leq i \leq m$. Each iterative scheme obtained its initial guess based on 200 power or Lanczos iterations, followed by a sequence of $T = 2,000$ (which can

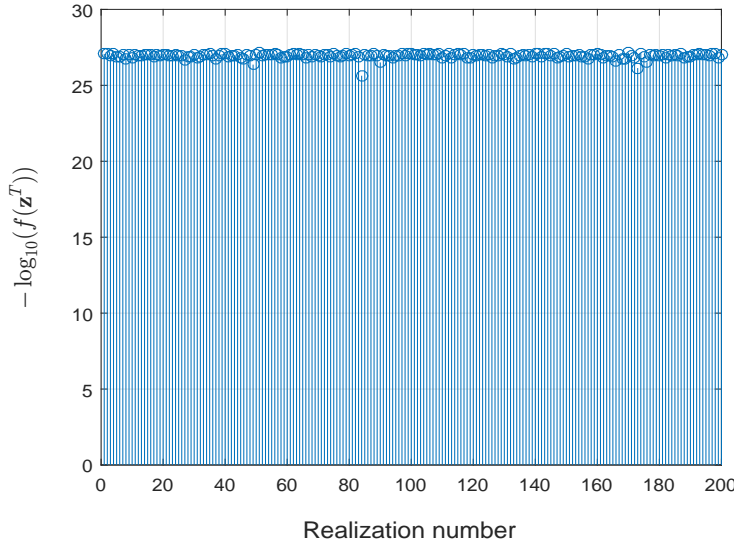


Fig. 2. Function value $L(\mathbf{z}^T)$ evaluated at the returned RAF estimate \mathbf{z}^T for 200 trials with $n = 2,000$ and $m = 2n - 1 = 3,999$.

be set smaller as the ratio m/n grows away from the limit of 2) gradient-type iterations. For reproducibility, the Matlab implementation of our RAF algorithm is publicly available at <https://gangumn.github.io/RAF/>.

To show the power of RAF in the high-dimensional regime, the function value $L(\mathbf{z})$ in (2) evaluated at the returned estimate \mathbf{z}^T (cf. Step 5 of Algorithm 1) for 200 MC realizations is plotted (in negative logarithmic scale) in Fig. 2, where the number of simulated noiseless measurements was set to be the information-theoretic limit, namely, $m = 2n - 1 = 3,999$ for $n = 2,000$. It is self-evident that our proposed RAF approach returns a solution of function value $L(\mathbf{z}^T)$ smaller than 10^{-25} in all 200 independent realizations even at this challenging information-theoretic limit condition. To the best of our knowledge, RAF is the first algorithm that empirically reconstructs any high-dimensional (say e.g., $n \geq 1,500$) signals exactly from an *optimal number* of random quadratic equations, which also provides a positive answer to the question posed easier in the Introduction.

The left panel in Fig. 3 further compares the empirical success rate of five schemes with the signal dimension being fixed at $n = 1,000$ while the ratio m/n increasing by 0.1 from 1 to 5. As clearly depicted by the plots, our RAF (the red plot) enjoys markedly improved performance over its competing alternatives. Moreover, it also achieves 100% perfect signal recovery as soon as m is about $2n$, where the others do not work (well). To numerically demonstrate the stability and robustness of RAF in the presence of additive noise, the right panel in Fig. 3 examines the normalized mean-square error $\text{NMSE} := \text{dist}^2(\mathbf{z}^T, \mathbf{x})/\|\mathbf{x}\|^2$ as a function of the signal-to-noise ratio (SNR) for m/n taking values $\{3, 4, 5\}$. The noise model $\psi_i = |\langle \mathbf{a}_i, \mathbf{x} \rangle| + \eta_i$ with $\boldsymbol{\eta} := [\eta_i]_{1 \leq i \leq m} \sim \mathcal{N}(\mathbf{0}, \sigma^2 \mathbf{I}_m)$ was simulated, where σ^2 was set such that certain $\text{SNR} := 10 \log_{10}(\|\mathbf{A}\mathbf{x}\|^2/m\sigma^2)$ values were achieved. For all choices of m (as small as $3n$ which is nearly minimal), the numerical experiments illustrate that the NMSE scales inversely proportional to the SNR, which corroborates the stability of our RAF approach.

To demonstrate the efficacy and scalability of RAF in real-world conditions, the last experiment entails the Galaxy image³ depicted by a three-way array $\mathbf{X} \in \mathbb{R}^{1,080 \times 1,920 \times 3}$, whose first two coordinates encode

³Downloaded from <http://pics-about-space.com/milky-way-galaxy>.

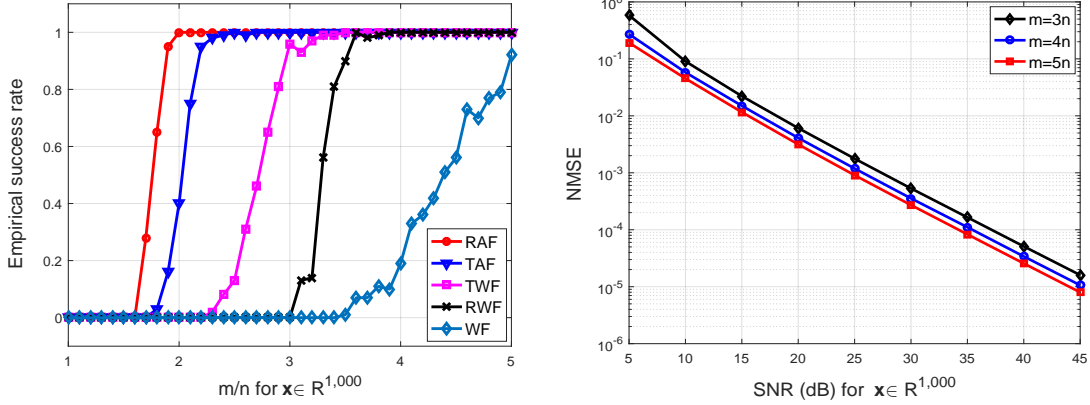


Fig. 3. Real-valued Gaussian model with $\mathbf{x} \in \mathbb{R}^{1,000}$: Empirical success rate (Left); and, NMSE vs. SNR (Right).

the pixel locations, and the third the RGB color bands. Consider the physically realizable CDP model with random masks [7]. Letting $\mathbf{x} \in \mathbb{R}^n$ ($n \approx 2 \times 10^6$) be a vectorization of a certain band of \mathbf{X} , the CDP model with K masks is $\psi^{(k)} = |\mathbf{F}\mathbf{D}^{(k)}\mathbf{x}|$, $1 \leq k \leq K$, where $\mathbf{F} \in \mathbb{C}^{n \times n}$ is a discrete Fourier transform matrix, and diagonal matrices $\mathbf{D}^{(k)}$ have their diagonal entries sampled uniformly at random from $\{1, -1, j, -j\}$ with $j := \sqrt{-1}$. Implementing $K = 4$ masks, each algorithm performs independently over each band 100 power iterations for an initial guess, which was refined by 100 gradient iterations. Recovered images of TAF (left) and RAF (right) are displayed in Fig. 4, whose relative errors were 1.0347 and 1.0715×10^{-3} , respectively. WF and TWF returned images of corresponding relative error 1.6870 and 1.4211, which are far away from the ground truth.

Regarding running times, RAF converges faster both in time and in the number of iterations required to achieve certain solution accuracy than TWF and WF in all simulated experiments, and it has comparable efficiency as TAF and RWF. All numerical experiments were implemented with MATLAB R2016a on an Intel CPU @ 3.4 GHz (32 GB RAM) computer.

V. PROOFS

To prove Theorem 1, this section establishes a few lemmas and the main ideas, whereas technical details are postponed to the Appendix for readability. It is clear from Algorithm 1 that the weighted maximal correlation initialization (cf. Step 3) and the reweighted gradient flow (cf. Step 4) distinguish themselves from those procedures in (T)WF [7], [14], TAF [36], and RWF [40]. Hence, new proof techniques to cope with the weighting in both the initialization and the gradient flow, as well as the nonsmoothness and nonconvexity of the amplitude-based least-squares functional are required. Nevertheless, part of the proof is built upon those in [7], [40], [36], [12].

The proof of Theorem 1 is based on two parts: Section V-A below corroborates guaranteed theoretical performance of the proposed initialization, which essentially achieves any given constant relative error as soon as the number of equations is on the order of the number of unknowns; that is, $m \geq c_1 n$ for some constant $c_1 > 0$. It is worth mentioning that we reserve c and its subscripted versions for absolute constants, and their values may vary with the context. Under the sample complexity of order $\mathcal{O}(n)$, Section V-B further shows that RAF converges to the true signal \mathbf{x} exponentially fast whenever the initial estimate lands within a relatively small-size neighborhood of \mathbf{x} defined by $\text{dist}(\mathbf{z}^0, \mathbf{x}) \leq (1/10)\|\mathbf{x}\|$.



Fig. 4. The recovered Milky Way Galaxy images after 100 truncated gradient iterations of TAF (Top); and after 100 reweighted gradient iterations of RAF (Bottom).

A. Weighted maximal correlation initialization

This section is devoted to developing theoretical guarantees for the novel initialization procedure, which is summarized in the following proposition.

Proposition 1. *For arbitrary $\mathbf{x} \in \mathbb{R}^n$, consider the noiseless measurements $\psi_i = |\mathbf{a}_i^* \mathbf{x}|$, $1 \leq i \leq m$. If $m \geq c_0|\mathcal{S}| \geq c_1 n$, then with probability exceeding $1 - c_3 e^{-c_2 m}$, the initial guess \mathbf{z}^0 obtained by the weighted maximal correlation method in Step 3 of Algorithm 1 satisfies*

$$\text{dist}(\mathbf{z}^0, \mathbf{x}) \leq \rho \|\mathbf{x}\| \quad (16)$$

for $\rho = 1/10$ (or any sufficiently small positive number). Here, $c_0, c_1, c_2, c_3 > 0$ are some absolute constants.

Due to the homogeneity of (16), it suffices to prove the result for the case of $\|\mathbf{x}\| = 1$. Assume first that the norm $\|\mathbf{x}\| = 1$ is also perfectly known, and \mathbf{z}^0 has already been scaled such that $\|\mathbf{z}^0\| = 1$. At the end of this proof, this approximation error between the actually employed norm estimate $\sqrt{\sum_{i=1}^m y_i/m}$ found based on the strong law of large numbers and the unknown norm $\|\mathbf{x}\| = 1$ will be taken care of. For independent Gaussian random measurement vectors $\mathbf{a}_i \sim \mathcal{N}(\mathbf{0}, \mathbf{I}_n)$ and arbitrary unit signal vector \mathbf{x} , there always exists an orthogonal transformation denoted by $\mathbf{U} \in \mathbb{R}^{n \times n}$ such that $\mathbf{x} = \mathbf{U}\mathbf{e}_1$. Since

$$|\langle \mathbf{a}_i, \mathbf{x} \rangle|^2 = |\langle \mathbf{a}_i, \mathbf{U}\mathbf{e}_1 \rangle|^2 = |\langle \mathbf{U}^* \mathbf{a}_i, \mathbf{e}_1 \rangle|^2 \stackrel{d}{=} |\langle \mathbf{a}_i, \mathbf{e}_1 \rangle|^2 \quad (17)$$

where $\stackrel{d}{=}$ means random quantities on both sides of the equality have the same distribution, it is thus without loss of generality to work with $\mathbf{x} = \mathbf{e}_1$.

Since the norm $\|\mathbf{x}\| = 1$ is assumed known, the weighted maximal correlation initialization in Step 3 finds the initial estimate $\mathbf{z}^0 = \tilde{\mathbf{z}}^0$ (the scaling factor is the exactly known norm 1 in this case) as the principal eigenvector of

$$\mathbf{Y} := \frac{1}{|\mathcal{S}|} \mathbf{B}^* \mathbf{B} = \frac{1}{|\mathcal{S}|} \sum_{i \in \mathcal{S}} \psi_i^\gamma \mathbf{a}_i \mathbf{a}_i^* \quad (18)$$

where $\mathbf{B} := [\psi_i^{\gamma/2} \mathbf{a}_i]_{i \in \mathcal{S}}$ is an $|\mathcal{S}| \times n$ matrix, and $\mathcal{S} \subsetneq \{1, 2, \dots, m\}$ includes the indices of the $|\mathcal{S}|$ largest entities among all modulus data $\{\psi_i\}_{1 \leq i \leq m}$. The following result is a modification of [36, Lemma 1], which is key to proving Proposition 1 and whose proof can be found in Section A in the Appendix.

Lemma 1. *Consider m noiseless measurements $\psi_i = |\mathbf{a}_i^* \mathbf{x}|$, $1 \leq i \leq m$. For arbitrary $\mathbf{x} \in \mathbb{R}^n$ of unity norm, the next result holds for all unit vectors $\mathbf{u} \in \mathbb{R}^n$ perpendicular to the vector \mathbf{x} ; that is, for all vectors $\mathbf{u} \in \mathbb{R}^n$ satisfying $\mathbf{u}^* \mathbf{x} = 0$ and $\|\mathbf{u}\| = 1$:*

$$\frac{1}{2} \|\mathbf{x} \mathbf{x}^* - \mathbf{z}^0 (\mathbf{z}^0)^*\|_F^2 \leq \frac{\|\mathbf{B} \mathbf{u}\|^2}{\|\mathbf{B} \mathbf{x}\|^2} \quad (19)$$

where $\mathbf{z}^0 = \tilde{\mathbf{z}}^0$ is given by

$$\tilde{\mathbf{z}}^0 := \arg \max_{\|\mathbf{z}\|=1} \frac{1}{|\mathcal{S}|} \mathbf{z}^* \mathbf{B}^* \mathbf{B} \mathbf{z}. \quad (20)$$

In the sequel, we start proving Proposition 1. The first step consists in upper-bounding the quantity on the right-hand-side of (19). To be specific, this task involves upper bounding its numerator, and lower bounding its denominator, which are summarized in Lemma 2 and Lemma 3 and whose proofs are deferred to Section B and Section C in the Appendix, accordingly.

Lemma 2. *In the setting of Lemma 1, if $|\mathcal{S}|/n \geq c_4$, then the next*

$$\|\mathbf{B} \mathbf{u}\|^2 \leq 1.01 \sqrt{2^\gamma / \pi} \Gamma(\gamma + 1/2) |\mathcal{S}| \quad (21)$$

holds with probability at least $1 - 2e^{-c_5 n}$, where $\Gamma(\cdot)$ is the Gamma function, and c_4, c_5 are certain universal constants.

Lemma 3. *In the setting of Lemma 1, the following holds with probability exceeding $1 - e^{-c_6 m}$:*

$$\|\mathbf{B} \mathbf{x}\|^2 \geq 0.99 |\mathcal{S}| [1 + \log(m/|\mathcal{S}|)] \geq 0.99 \times 1.14^\gamma |\mathcal{S}| [1 + \log(m/|\mathcal{S}|)] \quad (22)$$

provided that $m \geq c_0 |\mathcal{S}| \geq c_1 n$ for some absolute constants $c_0, c_1, c_6 > 0$.

Taking together the upper bound in (21) and the lower bound in (22), one arrives at

$$\frac{\|\mathbf{B} \mathbf{u}\|^2}{\|\mathbf{B} \mathbf{x}\|^2} \leq \frac{C}{1 + \log(m/|\mathcal{S}|)} \triangleq \kappa \quad (23)$$

where the constant $C := 1.02 \times 1.14^{-\gamma} \sqrt{2^\gamma / \pi} \Gamma(\gamma + 1/2)$ and which holds with probability at least $1 - 2e^{-c_5 n} - e^{-c_6 m}$, with the proviso that $m \geq c_0 |\mathcal{S}| \geq c_1 n$. Since $m = O(n)$, one can then rewrite the probability as $1 - c_3 e^{-c_2 m}$ for certain constants $c_2, c_3 > 0$. To have a sense of the size of C , taking our default value $\gamma = 0.5$ for instance gives rise to $C = 0.7854$.

It is clear that the bound κ in (23) can be rendered arbitrarily small by taking sufficiently large $m/|\mathcal{S}|$ values (while maintaining $|\mathcal{S}|/n$ to be some constant based on Lemma 3). With no loss of generality, let us work with $\kappa := 0.001$ in the following.

The wanted upper bound on the distance between the initialization \mathbf{z}^0 and the truth \mathbf{x} can be obtained based upon similar arguments found in [7, Section 7.8], which are delineated as follows. For unit vectors \mathbf{x} and \mathbf{z}^0 , recall from (48) that

$$|\mathbf{x}^* \mathbf{z}^0|^2 = \cos^2 \theta = 1 - \sin^2 \theta \geq 1 - \kappa, \quad (24)$$

where $0 \leq \theta \leq \pi/2$ denotes the angle between the spaces spanned by \mathbf{z}^0 and \mathbf{x} , therefore

$$\begin{aligned} \text{dist}^2(\mathbf{z}^0, \mathbf{x}) &\leq \|\mathbf{z}^0\|^2 + \|\mathbf{x}\|^2 - 2|\mathbf{x}^* \mathbf{z}^0| \\ &\leq (2 - 2\sqrt{1 - \kappa}) \|\mathbf{x}\|^2 \\ &\approx \kappa \|\mathbf{x}\|^2. \end{aligned} \quad (25)$$

As discussed prior to Lemma 1, the exact norm $\|\mathbf{x}\| = 1$ is generally not known, and one often scales the unit directional vector found in (20) by the estimate $\sqrt{\sum_{i=1}^m \psi_i^2/m}$. Next the approximation error between the estimated norm $\|\mathbf{z}^0\| = \sqrt{\sum_{i=1}^m \psi_i^2/m}$ and the true norm $\|\mathbf{x}\| = 1$ is accounted for. Recall from (20) that the direction of \mathbf{x} is estimated to be $\tilde{\mathbf{z}}^0$ (of unity norm). Using similar results in [7, Lemma 7.8 and Section 7.8], the following holds with high probability as long as the ratio m/n exceeds some numerical constant

$$\|\mathbf{z}^0 - \tilde{\mathbf{z}}^0\| = |\|\mathbf{z}^0\| - 1| \leq (1/20)\|\mathbf{x}\|. \quad (26)$$

Taking the inequalities in (25) and (26) together, it is safe to conclude that

$$\text{dist}(\mathbf{z}^0, \mathbf{x}) \leq \|\mathbf{z}^0 - \tilde{\mathbf{z}}^0\| + \text{dist}(\tilde{\mathbf{z}}^0, \mathbf{x}) \leq (1/10)\|\mathbf{x}\| \quad (27)$$

which confirms that the initial estimate obeys the relative error $\text{dist}(\mathbf{z}^0, \mathbf{x})/\|\mathbf{x}\| \leq 1/10$ for any $\mathbf{x} \in \mathbb{R}^n$ with probability $1 - c_3 e^{-c_2 m}$, provided that $m \geq c_0 |\mathcal{S}| \geq c_1 n$ for some numerical constants $c_0, c_1, c_2, c_3 > 0$.

B. Exact Phase Retrieval from Noiseless Data

It has been demonstrated that the initial estimate \mathbf{z}^0 obtained by means of the weighted maximal correlation initialization strategy has at most a constant relative error to the globally optimal solution \mathbf{x} , i.e., $\text{dist}(\mathbf{z}^0, \mathbf{x}) \leq (1/10)\|\mathbf{x}\|$. We demonstrate in the following that starting from such an initial estimate, the RAF iterates (in Step 4 of Algorithm 1) converge at a linear rate to the global optimum \mathbf{x} ; that is, $\text{dist}(\mathbf{z}^t, \mathbf{x}) \leq (1/10)c^t\|\mathbf{x}\|$ for some constant $0 < c < 1$ depending on the step size $\mu > 0$, the weighting parameter β , and the data $\{(\mathbf{a}_i; \psi_i)\}_{1 \leq i \leq m}$. This constitutes the second part of the proof of Theorem 1. Toward this end, it suffices to show that the iterative updates of RAF is locally contractive within a relatively small neighboring region of the truth \mathbf{x} . Instead of directly coping with the moments in the weights, we establish a conservative result based directly on [36] and [40]. Recall first that our gradient flow uses the reweighted gradient

$$\nabla \ell_{\text{rw}}(\mathbf{z}) := \frac{1}{m} \sum_{i=1}^m w_i \left(\mathbf{a}_i^* \mathbf{z} - \psi_i \frac{\mathbf{a}_i^* \mathbf{z}}{|\mathbf{a}_i^* \mathbf{z}|} \right) \mathbf{a}_i = \frac{1}{m} \sum_{i=1}^m w_i \left(\mathbf{a}_i^* \mathbf{z} - |\mathbf{a}_i^* \mathbf{x}| \frac{\mathbf{a}_i^* \mathbf{z}}{|\mathbf{a}_i^* \mathbf{z}|} \right) \mathbf{a}_i \quad (28)$$

with weights

$$w_i = \frac{1}{1 + \beta / (|\mathbf{a}_i^* \mathbf{z}| / |\mathbf{a}_i^* \mathbf{x}|)}, \quad 1 \leq i \leq m \quad (29)$$

in which the dependence on the iterate index t is ignored for notational brevity.

Proposition 2 (Local error contraction). *For arbitrary $\mathbf{x} \in \mathbb{R}^n$, consider m noise-free measurements $\psi_i = |\mathbf{a}_i^* \mathbf{x}|$, $1 \leq i \leq m$. There exist some numerical constants $c_1, c_2, c_3 > 0$, and $0 < \nu < 1$ such that the following holds with probability exceeding $1 - c_3 e^{-c_2 m}$*

$$\text{dist}^2(\mathbf{z} - \mu \nabla \ell_{\text{rw}}(\mathbf{z}), \mathbf{x}) \leq (1 - \nu) \text{dist}^2(\mathbf{z}, \mathbf{x}) \quad (30)$$

for all $\mathbf{x}, \mathbf{z} \in \mathbb{R}^n$ obeying $\text{dist}(\mathbf{z}, \mathbf{x}) \leq (1/10) \|\mathbf{x}\|$, provided that $m \geq c_1 n$ and that the constant step size $\mu \leq \mu_0$, where the numerical constant μ_0 depends on the parameter $\beta > 0$ and data $\{(\mathbf{a}_i; \psi_i)\}_{1 \leq i \leq m}$.

Proposition 2 suggests that the distance of RAF's successive iterates to the global optimum \mathbf{x} decreases monotonically once the algorithm's iterate \mathbf{z}^t enters a small neighboring region around the truth \mathbf{x} . This small-size neighborhood is commonly known as the *basin of attraction*, and has been widely discussed in recent nonconvex optimization contributions; see e.g., [14], [40], [36]. Expressed differently, RAF's iterates will stay within the region and will be attracted towards \mathbf{x} exponentially fast as soon as it lands within the basin of attraction. To substantiate Proposition 2, recall the useful analytical tool of the local regularity condition [7], which plays a key role in establishing linear convergence of iterative procedures to the global optimum in [7], [14], [40], [36], [35], [11], [39].

For RAF, the reweighted gradient $\nabla \ell_{\text{rw}}(\mathbf{z})$ in (28) is said to obey the local regularity condition, or LRC(μ, λ, ϵ) for some constant $\lambda > 0$, if the following inequality

$$\langle \nabla \ell_{\text{rw}}(\mathbf{z}), \mathbf{h} \rangle \geq \frac{\mu}{2} \|\nabla \ell_{\text{rw}}(\mathbf{z})\|^2 + \frac{\lambda}{2} \|\mathbf{h}\|^2 \quad (31)$$

holds for all $\mathbf{z} \in \mathbb{R}^n$ such that $\|\mathbf{h}\| = \|\mathbf{z} - \mathbf{x}\| \leq \epsilon \|\mathbf{x}\|$ for some constant $0 < \epsilon < 1$, where the ball given by $\|\mathbf{z} - \mathbf{x}\| \leq \epsilon \|\mathbf{x}\|$ is the so-termed *basin of attraction*.

Realizing $\mathbf{h} := \mathbf{z} - \mathbf{x}$, algebraic manipulations in conjunction with the regularity property (31) confirms

$$\begin{aligned} \text{dist}^2(\mathbf{z} - \mu \nabla \ell_{\text{rw}}(\mathbf{z}), \mathbf{x}) &= \|\mathbf{z} - \mu \nabla \ell_{\text{rw}}(\mathbf{z}) - \mathbf{x}\|^2 \\ &= \|\mathbf{h}\|^2 - 2\mu \langle \mathbf{h}, \nabla \ell_{\text{rw}}(\mathbf{z}) \rangle + \|\mu \nabla \ell_{\text{rw}}(\mathbf{z})\|^2 \end{aligned} \quad (32)$$

$$\begin{aligned} &\leq \|\mathbf{h}\|^2 - 2\mu \left(\frac{\mu}{2} \|\nabla \ell_{\text{rw}}(\mathbf{z})\|^2 + \frac{\lambda}{2} \|\mathbf{h}\|^2 \right) + \|\mu \nabla \ell_{\text{rw}}(\mathbf{z})\|^2 \\ &= (1 - \lambda\mu) \|\mathbf{h}\|^2 = (1 - \lambda\mu) \text{dist}^2(\mathbf{z}, \mathbf{x}) \end{aligned} \quad (33)$$

for all points \mathbf{z} adhering to $\|\mathbf{h}\| \leq \epsilon \|\mathbf{x}\|$. It is self-evident that if the regularity condition LRC(μ, λ, ϵ) can be established for RAF, our ultimate goal of proving the local error contraction in (30) follows straightforwardly upon setting $\nu := \lambda\mu$.

1) *Proof of the local regularity condition in (31):* The first step of proving the local regularity condition in (31) is to control the size of the reweighted gradient $\nabla \ell_{\text{rw}}(\mathbf{z})$, i.e., to upper bound the last term in (32). To start, let rewrite the reweighted gradient in a compact matrix-vector representation

$$\nabla \ell_{\text{rw}}(\mathbf{z}) = \frac{1}{m} \sum_{i=1}^m w_i \left(\mathbf{a}_i^* \mathbf{z} - |\mathbf{a}_i^* \mathbf{x}| \frac{\mathbf{a}_i^* \mathbf{z}}{|\mathbf{a}_i^* \mathbf{z}|} \right) \mathbf{a}_i \triangleq \frac{1}{m} \text{diag}(\mathbf{w}) \mathbf{A} \mathbf{v} \quad (34)$$

where $\text{diag}(\mathbf{w}) \in \mathbb{R}^{n \times n}$ is a diagonal matrix holding in order entries of $\mathbf{w} := [w_1 \dots w_m]^* \in \mathbb{R}^m$ on its main diagonal, and $\mathbf{v} := [v_1 \dots v_m]^* \in \mathbb{R}^m$ with $v_i := \mathbf{a}_i^* \mathbf{z} - |\mathbf{a}_i^* \mathbf{x}| \frac{\mathbf{a}_i^* \mathbf{z}}{|\mathbf{a}_i^* \mathbf{z}|}$. Based on the definition of the induced matrix 2-norm (or the matrix spectral norm), it is easy to check that

$$\|\nabla \ell_{\text{rw}}(\mathbf{z})\| = \left\| \frac{1}{m} \text{diag}(\mathbf{w}) \mathbf{A} \mathbf{v} \right\|$$

$$\begin{aligned} &\leq \frac{1}{m} \|\text{diag}(\mathbf{w})\| \cdot \|\mathbf{A}\| \cdot \|\mathbf{v}\| \\ &\leq \frac{1 + \delta'}{\sqrt{m}} \|\mathbf{v}\| \end{aligned} \quad (35)$$

where we have used the inequalities $\|\text{diag}(\mathbf{w})\| \leq 1$ due to $w_i \leq 1$ for all $1 \leq i \leq m$, and $\|\mathbf{A}\| \leq (1 + \delta')\sqrt{m}$ for some constant $\delta' > 0$ according to [32, Theorem 5.32], provided that m/n is sufficiently large.

The task therefore remains to bound $\|\mathbf{v}\|$ in (35), which is addressed next. To this end, notice that

$$\begin{aligned} \|\mathbf{v}\|^2 &= \sum_{i=1}^m \left(\mathbf{a}_i^* \mathbf{z} - |\mathbf{a}_i^* \mathbf{x}| \frac{\mathbf{a}_i^* \mathbf{z}}{|\mathbf{a}_i^* \mathbf{z}|} \right)^2 \leq \sum_{i=1}^m (|\mathbf{a}_i^* \mathbf{z}| - |\mathbf{a}_i^* \mathbf{x}|)^2 \\ &\leq \sum_{i=1}^m (\mathbf{a}_i^* \mathbf{z} - \mathbf{a}_i^* \mathbf{x})^2 \\ &= \sum_{i=1}^m (\mathbf{a}_i^* \mathbf{h})^2 \leq (1 + \delta'')^2 m \|\mathbf{h}\|^2 \end{aligned} \quad (36)$$

for some numerical constant $\delta'' > 0$, where the last can be obtained using [8, Lemma 3.1] and which holds with probability at least $1 - e^{-c_2 m}$ as long as $m > c_1 n$ holds true.

Combining the results in (35) and (36) and taking $\delta > 0$ larger than the constant $(1 + \delta')(1 + \delta'') - 1$, the size of $\nabla \ell_{\text{rw}}(\mathbf{z})$ can be bounded as follows

$$\|\nabla \ell_{\text{rw}}(\mathbf{z})\| \leq (1 + \delta) \|\mathbf{h}\| \quad (37)$$

which holds with probability $1 - e^{-c_2 m}$, with a proviso that m/n exceeds some numerical constant $c_7 > 0$. This result indeed asserts that the reweighted gradient of the objective function $L(\mathbf{z})$ or the search direction employed in our RAF algorithm is well behaved, implying that the function value along the iterates does not change too much.

In order to prove the LRC, it suffices to show that the reweighted gradient $\nabla \ell_{\text{rw}}(\mathbf{z})$ ensures sufficient descent, that is, there exists a numerical constant $c > 0$ such that along the search direction $\nabla \ell_{\text{rw}}(\mathbf{z})$ the following uniform lower bound holds

$$\langle \nabla \ell_{\text{rw}}(\mathbf{z}), \mathbf{h} \rangle \geq c \|\mathbf{h}\|^2 \quad (38)$$

which will be addressed next. Formally, this can be summarized in the following proposition, whose proof is deferred to Appendix D.

Proposition 3. *Fixing any sufficiently small constant $\epsilon > 0$, consider the noise-free measurements $\psi_i = |\mathbf{a}_i^* \mathbf{x}|$, $1 \leq i \leq m$. There exist some numerical constants $c_1, c_2, c_3 > 0$ such that the following holds with probability at least $1 - c_3 e^{-c_2 m}$:*

$$\langle \mathbf{h}, \nabla \ell_{\text{rw}}(\mathbf{z}) \rangle \geq \left[\frac{1 - \zeta_1 - \epsilon}{1 + \beta(1 + \eta)} - 2(\zeta_2 + \epsilon) - \frac{2(0.1271 - \zeta_2 + \epsilon)}{1 + \beta/k} \right] \|\mathbf{h}\|^2 \quad (39)$$

for all $\mathbf{x}, \mathbf{z} \in \mathbb{R}^n$ obeying $\|\mathbf{h}\| \leq \frac{1}{10} \|\mathbf{x}\|$, provided that $m/n > c_1$, and that $\beta \geq 0$ is small enough.

Taking the results in (39) and (37) together back to (31), one concludes that the local regularity condition holds for μ and λ obeying the following

$$\frac{1 - \zeta_1 - \epsilon}{1 + \beta(1 + \eta)} - 2(\zeta_2 + \epsilon) - \frac{2(0.1271 - \zeta_2 + \epsilon)}{1 + \beta/k} \geq \frac{\mu}{2}(1 + \delta)^2 + \frac{\lambda}{2}. \quad (40)$$

For instance, take $\beta = 2$, $k = 5$, $\eta = 0.5$, and $\epsilon = 0.001$, we have $\zeta_1 = 0.8897$ and $\zeta_2 = 0.0213$, thus confirming that $\langle \ell_{\text{rw}}(\mathbf{z}), \mathbf{h} \rangle \geq 0.1065 \|\mathbf{h}\|^2$. Setting further $\delta = 0.001$ leads to

$$0.1065 \geq 0.501\mu + 0.5\lambda \quad (41)$$

which concludes the proof of the local regularity condition in (31). The local error contraction in (30) follows directly from substituting the local regularity condition into (33), hence validating Proposition 2.

VI. CONCLUSIONS

This paper put forth a linear-time algorithm termed reweighted amplitude flow (RAF) for solving systems of random quadratic equations. Our novel procedure effects two consecutive stages, namely, a weighted maximal correlation initialization that is attainable based upon a few power or Lanczos iterations, and a sequence of simple iteratively reweighted generalized gradient iterations for the nonconvex nonsmooth least-squares loss function. Our RAF approach is conceptually simple, easy-to-implement, as well as numerically scalable and effective. It was also demonstrated to achieve the optimal sample and computational complexity orders. Substantial numerical tests using both synthetic data and real images corroborated the superior performance of RAF over state-of-the-art iterative solvers. Empirically, RAF solves a set of random quadratic equations in the high-dimensional regime with large probability so long as a unique solution exists, where the number m of equations in the real-valued Gaussian case can be as small as $2n - 1$ with n being the number of unknowns to be recovered.

Future research extensions include studying robust and/or sparse phase retrieval and (semi-definite) matrix recovery by means of (stochastic) reweighted amplitude flow counterparts [37], [16], [39], [13], [24]. Exploiting the possibility of leveraging suitable (re)weighting regularization to improve empirical performance of other nonconvex iterative procedures such as [16], [39], [11] is worth investigating as well.

Acknowledgments

The authors would like to thank John C. Duchi for his helpful feedback on our initialization.

APPENDIX

By homogeneity of (1), it suffices to work with the case where $\|\mathbf{x}\| = 1$.

A. Proof of Lemma 1

It is easy to check that

$$\begin{aligned} \frac{1}{2} \|\mathbf{x}\mathbf{x}^* - \mathbf{z}^0(\mathbf{z}^0)^*\|_F^2 &= \frac{1}{2} \|\mathbf{x}\|^4 + \frac{1}{2} \|\mathbf{z}^0\|^4 - |\mathbf{x}^* \mathbf{z}^0|^2 \\ &= 1 - |\mathbf{x}^* \mathbf{z}^0|^2 \\ &= 1 - \cos^2 \theta \end{aligned} \quad (42)$$

where $0 \leq \theta \leq \pi/2$ denotes the angle between the hyperplanes spanned by \mathbf{x} and \mathbf{z}^0 . Letting $(\mathbf{z}^0)^\perp \in \mathbb{R}^n$ be a unit vector orthogonal to \mathbf{z}^0 and have a nonnegative inner-product with \mathbf{x} , then \mathbf{x} can be uniquely expressed as a linear combination of \mathbf{z}^0 and $(\mathbf{z}^0)^\perp$, yielding

$$\mathbf{x} = \mathbf{z}^0 \cos \theta + (\mathbf{z}^0)^\perp \sin \theta. \quad (43)$$

Likewise, introduce the unit vector \mathbf{x}^\perp to be orthogonal to \mathbf{x} and to have a nonnegative inner-product with $(\mathbf{z}^0)^\perp$. Therefore, \mathbf{x}^\perp can be uniquely written as

$$\mathbf{x}^\perp := -\mathbf{z}^0 \sin \theta + (\mathbf{z}^0)^\perp \cos \theta. \quad (44)$$

Recall from (20) (after ignoring the normalization factor $1/|\mathcal{S}|$) that \mathbf{z}^0 is the solution to the principal component analysis (PCA) problem

$$\mathbf{z}^0 := \arg \max_{\|\mathbf{z}\|=1} \mathbf{z}^* \mathbf{B}^* \mathbf{B} \mathbf{z}. \quad (45)$$

Therefore, it holds that $\mathbf{B}^* \mathbf{B} \mathbf{z}^0 = \lambda_1 \mathbf{z}^0$, where $\lambda_1 > 0$ is the largest eigenvalue of $\mathbf{B}^* \mathbf{B}$. Multiplying (43) and (44) by \mathbf{B} from the left gives rise to

$$\mathbf{Bx} = \mathbf{Bz}^0 \cos \theta + \mathbf{B}(\mathbf{z}^0)^\perp \sin \theta, \quad (46a)$$

$$\mathbf{Bx}^\perp = -\mathbf{Bz}^0 \sin \theta + \mathbf{B}(\mathbf{z}^0)^\perp \cos \theta. \quad (46b)$$

Taking the 2-norm square of both sides in (46a) and (46b) yields

$$\|\mathbf{Bx}\|^2 = \|\mathbf{Bz}^0\|^2 \cos^2 \theta + \|\mathbf{B}(\mathbf{z}^0)^\perp\|^2 \sin^2 \theta, \quad (47a)$$

$$\|\mathbf{Bx}^\perp\|^2 = \|\mathbf{Bz}^0\|^2 \sin^2 \theta + \|\mathbf{B}(\mathbf{z}^0)^\perp\|^2 \cos^2 \theta, \quad (47b)$$

where the cross-terms disappear due to $(\mathbf{z}^0)^* \mathbf{B}^* \mathbf{B}(\mathbf{z}^0)^\perp = \lambda_1 (\mathbf{z}^0)^* (\mathbf{z}^0)^\perp = 0$ according to the definition of $(\mathbf{z}^0)^\perp$.

With the relationships established in (47), construct now the following

$$\begin{aligned} & \|\mathbf{Bx}\|^2 \sin^2 \theta - \|\mathbf{Bx}^\perp\|^2 \\ &= (\|\mathbf{Bz}^0\|^2 \cos^2 \theta + \|\mathbf{B}(\mathbf{z}^0)^\perp\|^2 \sin^2 \theta) \sin^2 \theta - (\|\mathbf{Bz}^0\|^2 \sin^2 \theta + \|\mathbf{B}(\mathbf{z}^0)^\perp\|^2 \cos^2 \theta) \\ &= (\|\mathbf{Bz}^0\|^2 \cos^2 \theta - \|\mathbf{Bz}^0\|^2 + \|\mathbf{B}(\mathbf{z}^0)^\perp\|^2 \sin^2 \theta) \sin^2 \theta - \|\mathbf{B}(\mathbf{z}^0)^\perp\|^2 \cos^2 \theta \\ &= (\|\mathbf{B}(\mathbf{z}^0)^\perp\|^2 - \|\mathbf{Bz}^0\|^2) \sin^4 \theta - \|\mathbf{B}(\mathbf{z}^0)^\perp\|^2 \cos^2 \theta \\ &\leq 0 \end{aligned}$$

where $\mathbf{B}^* \mathbf{B} \succeq \mathbf{0}$, so $\|\mathbf{B}(\mathbf{z}^0)^\perp\|^2 - \|\mathbf{Bz}^0\|^2 \leq 0$ holds for any unit vector $(\mathbf{z}^0)^\perp \in \mathbb{R}^n$ because \mathbf{z}^0 maximizes the term in (20), hence yielding

$$\sin^2 \theta = 1 - \cos^2 \theta \leq \frac{\|\mathbf{Bx}^\perp\|^2}{\|\mathbf{Bx}\|^2}. \quad (48)$$

Plugging (42) into above, (19) follows directly from setting $\mathbf{u} = \mathbf{x}^\perp$.

B. Proof of Lemma 2

Let $\{\mathbf{b}_i^*\}_{1 \leq i \leq |\mathcal{S}|}$ denote rows of $\mathbf{B} \in \mathbb{R}^{|\mathcal{S}| \times n}$, which are obtained by scaling rows of $\mathbf{A}_{\mathcal{S}} := \{\mathbf{a}_i^*\}_{i \in \mathcal{S}} \in \mathbb{R}^{|\mathcal{S}| \times n}$ by weights $\{w_i = \psi_i^{\gamma/2}\}_{i \in \mathcal{S}}$ [cf. (18)]. Since $\mathbf{x} = \mathbf{e}_1$, then $\psi = |\mathbf{Ae}_1| = |\mathbf{A}_1|$, namely, the index set \mathcal{S} depends solely on the first column of \mathbf{A} , and is independent of the other columns of \mathbf{A} . In this direction, partition accordingly $\mathbf{A}^{\mathcal{S}} := [\mathbf{A}_1^{\mathcal{S}} \ \mathbf{A}_r^{\mathcal{S}}]$, where $\mathbf{A}_1^{\mathcal{S}} \in \mathbb{R}^{|\mathcal{S}| \times 1}$ denotes the first column of $\mathbf{A}^{\mathcal{S}}$, and $\mathbf{A}_r^{\mathcal{S}} \in \mathbb{R}^{|\mathcal{S}| \times (n-1)}$ collects the remaining ones. Likewise, partition $\mathbf{B} = [\mathbf{B}_1 \ \mathbf{B}_r]$ with $\mathbf{B}_1 \in \mathbb{R}^{|\mathcal{S}| \times 1}$ and $\mathbf{B}_r \in \mathbb{R}^{|\mathcal{S}| \times (n-1)}$. By the argument above, rows of $\mathbf{A}^{\mathcal{S}}$ are mutually independent, and they follow i.i.d. Gaussian distribution with mean $\mathbf{0}$ and covariance matrix \mathbf{I}_{n-1} . Furthermore, the weights $\psi_i^{\gamma/2} = |\mathbf{a}_i^* \mathbf{e}_1|^{\gamma/2} = |a_{i,1}|^{\gamma/2}$, $\forall i \in \mathcal{S}$ are also independent of the entries in $\mathbf{A}^{\mathcal{S}}$. As a consequence, rows of \mathbf{B}_r are mutually independent of each other, and one can explicitly write its i -th row as $\mathbf{b}_{r,i} = |\mathbf{a}_{[i]}^* \mathbf{e}_1|^{\gamma/2} \mathbf{a}_{[i],\setminus 1} = |a_{[i],1}|^{\gamma/2} \mathbf{a}_{[i],\setminus 1}$, where $\mathbf{a}_{[i],\setminus 1} \in \mathbb{R}^{n-1}$ is obtained through removing the first entry of $\mathbf{a}_{[i]}$. It is easy to verify that $\mathbb{E}[\mathbf{b}_{r,i}] = \mathbf{0}$, and $\mathbb{E}[\mathbf{b}_{r,i} \mathbf{b}_{r,i}^*] = C_\gamma \mathbf{I}_{n-1}$, where the constant $C_\gamma := \sqrt{2^\gamma / \pi \Gamma(\gamma+1/2)} \|\mathbf{x}\|^\gamma = \sqrt{2^\gamma / \pi \Gamma(\gamma+1/2)}$, and $\Gamma(\cdot)$ is the Gamma function.

Given $\mathbf{x}^* \mathbf{x}^\perp = \mathbf{e}_1^* \mathbf{x}^\perp = 0$, one can write $\mathbf{x}^\perp = [0 \ \mathbf{r}^*]^*$ with any unit vector $\mathbf{r} \in \mathbb{R}^{n-1}$, hence

$$\|\mathbf{B}\mathbf{x}^\perp\|^2 = \|\mathbf{B}[0 \ \mathbf{r}^*]^*\|^2 = \|\mathbf{B}_r \mathbf{r}\|^2 \quad (49)$$

with independent subgaussian rows $\mathbf{b}_{r,i} = |a_{j,1}|^{\gamma/2} \mathbf{a}_{j,\setminus 1}$ if $0 \leq \gamma \leq 1$. Standard concentration results on the sum of random positive semi-definite matrices composed of independent non-isotropic subgaussian rows [32, Remark 5.40.1] assert that

$$\left\| \frac{1}{|\mathcal{S}|} \mathbf{B}_r^* \mathbf{B}_r - C_\gamma \mathbf{I}_{n-1} \right\| \leq \delta \quad (50)$$

holds with probability at least $1 - 2e^{-c_5 n}$ provided that $|\mathcal{S}|/n$ is larger than some positive constant. Here, $\delta > 0$ is a numerical constant that can take arbitrarily small values, and $c_5 > 0$ is a constant depending on δ . With no loss of generality, take $\delta := 0.01C_\gamma$ in (50). For any unit vector $\mathbf{r} \in \mathbb{R}^{n-1}$, the following holds with probability at least $1 - 2e^{-c_5 n}$

$$\left\| \frac{1}{|\mathcal{S}|} \mathbf{r}^* \mathbf{B}_r^* \mathbf{B}_r \mathbf{r} - C_\gamma \mathbf{r}^* \mathbf{r} \right\| \leq \delta \mathbf{r}^* \mathbf{r} = \delta \quad (51)$$

or

$$\|\mathbf{B}_r \mathbf{r}\|^2 = \mathbf{r}^* \mathbf{B}_r^* \mathbf{B}_r \mathbf{r} \leq 1.01C_\gamma |\mathcal{S}|. \quad (52)$$

Taking the last back to (49) confirms that

$$\|\mathbf{B}\mathbf{x}^\perp\|^2 \leq 1.01C_\gamma |\mathcal{S}| \quad (53)$$

holds with probability at least $1 - 2e^{-c_5 n}$ if $|\mathcal{S}|/n$ exceeds some constant. Note that c_5 depends on the maximum subgaussian norm of the rows \mathbf{b}_i in \mathbf{B}_r , and we assume without loss of generality $c_5 \geq 1/2$. Therefore, one confirms that the numerator $\|\mathbf{B}\mathbf{u}\|^2$ in (19) is upper bounded via replacing \mathbf{x}^\perp with \mathbf{u} in (53).

C. Proof of Lemma 3

This section is devoted to obtaining a meaningful lower bound for the denominator $\|\mathbf{B}\mathbf{x}\|^2$ in (22). Note first that

$$\|\mathbf{B}\mathbf{x}\|^2 = \sum_{i=1}^{|\mathcal{S}|} \|\mathbf{b}_i^* \mathbf{x}\|^2 = \sum_{i=1}^{|\mathcal{S}|} \psi_{[i]}^\gamma |a_{[i]}^* \mathbf{x}|^2 = \sum_{i=1}^{|\mathcal{S}|} |a_{[i]}^* \mathbf{x}|^{2+\gamma}.$$

Taking without loss of generality $\mathbf{x} = \mathbf{e}_1$, the term on the right side of the last equality reduces to

$$\|\mathbf{B}\mathbf{x}\|^2 = \sum_{i=1}^{|\mathcal{S}|} |a_{[i],1}|^{2+\gamma}. \quad (54)$$

Since $a_{[i],1}$ follows the standard normal distribution, the probability density function (pdf) of random variables $|a_{[i],1}|^{2+\gamma}$ can be given in closed form as

$$p(t) = \sqrt{\frac{2}{\pi}} \cdot \frac{1}{2+\gamma} t^{-\frac{1+\gamma}{2+\gamma}} e^{-\frac{1}{2}t^{\frac{2}{2+\gamma}}}, \quad t > 0 \quad (55)$$

which is rather complicated and whose cumulative density function (cdf) does not come in closed-form in general. Therefore, instead of dealing with the pdf in (55) directly, we shall take a different route by deriving a lower bound that is a bit looser yet suffices for our purpose, which is detailed as follows.

Since $|a_{[|\mathcal{S}|],1}| \leq \dots \leq |a_{[2],1}| \leq |a_{[1],1}|$, then it holds for all $1 \leq i \leq |\mathcal{S}|$ that $|a_{[i],1}|^{2+\gamma} \geq |a_{[|\mathcal{S}|],1}|^\gamma a_{[i],1}^2$, therefore yielding

$$\|\mathbf{B}\mathbf{x}\|^2 = \sum_{i=1}^{|\mathcal{S}|} |a_{[i],1}|^{2+\gamma} \geq |a_{[|\mathcal{S}|],1}|^\gamma \sum_{i=1}^{|\mathcal{S}|} a_{[i],1}^2. \quad (56)$$

Hence, we next demonstrate that deriving a lower bound for $\|\mathbf{B}\mathbf{x}\|^2$ suffices to derive a lower bound for the summation on the right hand side above. The latter can be achieved by appealing to a result in [36, Lemma 3], which for completeness is included in the following.

Lemma 4. *For arbitrary unit vector $\mathbf{x} \in \mathbb{R}^n$, let $\psi_i = |\mathbf{a}_i^* \mathbf{x}|$, $1 \leq i \leq m$ be m noiseless measurements. Then with probability at least $1 - e^{-c_2 m}$, the following holds:*

$$\sum_{i=1}^{|\mathcal{S}|} a_{[i],1}^2 \geq 0.99 |\mathcal{S}| [1 + \log(m/|\mathcal{S}|)] \quad (57)$$

provided that $m \geq c_0 |\mathcal{S}| \geq c_1 n$ for some numerical constants $c_0, c_1, c_2 > 0$.

Combining the results in Lemma 4 and (56) together, one further establishes that

$$\|\mathbf{B}\mathbf{x}\|^2 \geq |a_{[|\mathcal{S}|],1}|^\gamma \sum_{i=1}^{|\mathcal{S}|} a_{[i],1}^2 \geq |a_{[|\mathcal{S}|],1}|^\gamma \cdot 0.99 |\mathcal{S}| [1 + \log(m/|\mathcal{S}|)]. \quad (58)$$

The task remains to estimate the size of $|a_{[|\mathcal{S}|],1}|$, which we recall is the $|\mathcal{S}|$ -th largest among the m independent realizations $\{\psi_i = |a_{i,1}|\}_{1 \leq i \leq m}$. Taking $\gamma = -1$ in (55) gives the pdf of the half-normal distribution

$$p(t) = \sqrt{\frac{2}{\pi}} e^{-\frac{1}{2}t^2}, \quad t > 0 \quad (59)$$

whose corresponding cdf is

$$F(\tau) = \text{erf}(\tau/\sqrt{2}). \quad (60)$$

Setting $F(\tau_{|\mathcal{S}|}) := 1 - |\mathcal{S}|/m$ or using the complementary cdf $|\mathcal{S}|/m := \text{erfc}(\tau/\sqrt{2})$ based on the complementary error function gives rise to an estimate of the size of the $|\mathcal{S}|$ -th largest [or equivalently, the $(m - |\mathcal{S}|)$ -th smallest] entry in the m realizations, namely

$$\tau_{|\mathcal{S}|} = \sqrt{2} \text{erfc}^{-1}(|\mathcal{S}|/m) \quad (61)$$

where $\text{erfc}^{-1}(\cdot)$ represents the inverse complementary error function. In the sequel, we show that the deviation of the $|\mathcal{S}|$ -th largest realization $\psi_{|\mathcal{S}|}$ from its expected value $\tau_{|\mathcal{S}|}$ found above is bounded with high probability.

For random variable $\psi = |a|$ with a obeying the standard Gaussian distribution, consider the event $\psi \leq \tau_{|\mathcal{S}|} - \delta$ for fixed constant $\delta > 0$. Define the indicator random variable $\chi = \mathbb{1}_{\{\psi \leq \tau_{|\mathcal{S}|} - \delta\}}$, whose expectation can be obtained by substituting $\tau = \tau_{|\mathcal{S}|} - \delta$ into the pdf in (60)

$$\mathbb{E}[\chi] = \text{erf}(\tau_{|\mathcal{S}|} - \delta/\sqrt{2}). \quad (62)$$

Consider now the m independent copies $\{\chi_i = \mathbb{1}_{\{\psi_i \leq \tau_{|\mathcal{S}|} - \delta\}}\}_{1 \leq i \leq m}$ of χ , and the following holds

$$\mathbb{P}(\psi_{|\mathcal{S}|} \leq \tau_{|\mathcal{S}|} - \delta) = \mathbb{P}\left(\sum_{i=1}^m \chi_i \leq m - |\mathcal{S}|\right)$$

$$= \mathbb{P}\left(\frac{1}{m} \sum_{i=1}^m (\chi_i - \mathbb{E}[\chi_i]) \leq 1 - \frac{|\mathcal{S}|}{m} - \mathbb{E}[\chi_i]\right). \quad (63)$$

Clearly, random variables χ_i are bounded, so they are sub-gaussian [32]. For notational brevity, let $t := 1 - |\mathcal{S}|/m - \mathbb{E}[\chi_i] = 1 - |\mathcal{S}|/m - \text{erf}(\tau_{|\mathcal{S}|} - \delta/\sqrt{2})$. Appealing to a large deviation inequality for sums of independent sub-gaussian random variables, one establishes that

$$\mathbb{P}(\psi_{|\mathcal{S}|} \leq \tau_{|\mathcal{S}|} - \delta) = \mathbb{P}\left(\frac{1}{m} \sum_{i=1}^m (\chi_i - \mathbb{E}[\chi_i]) \leq 1 - \frac{|\mathcal{S}|}{m} - \mathbb{E}[\chi_i]\right) \leq e^{-c_5 m t^2} \quad (64)$$

where $c_5 > 0$ is some absolute constant. On the other hand, using the definition of the error function and properties of integration gives rise to

$$t = 1 - |\mathcal{S}|/m - \text{erf}(\tau_{|\mathcal{S}|} - \delta/\sqrt{2}) = \frac{2}{\sqrt{\pi}} \int_{(\tau_{|\mathcal{S}|} - \delta)/\sqrt{2}}^{\tau_{|\mathcal{S}|}/\sqrt{2}} e^{-s^2} ds \geq \sqrt{\frac{2}{\pi}} \delta e^{-\frac{\tau_{|\mathcal{S}|}^2}{2}} \geq \sqrt{\frac{2}{\pi}} \delta. \quad (65)$$

Taking the results in (64) and (65) together, one concludes that fixing any constant $\delta > 0$, the following holds with probability at least $1 - e^{-c_2 m}$:

$$\psi_{|\mathcal{S}|} \geq \tau_{|\mathcal{S}|} - \delta \geq \sqrt{2} \operatorname{erfc}^{-1}(|\mathcal{S}|/m) - \delta$$

where the constant $c_2 := 2/\pi \cdot c_5 \delta^2$. Furthermore, choosing without loss of generality $\delta := 0.01 \tau_{|\mathcal{S}|}$ above leads to $\psi_{|\mathcal{S}|} \geq 1.4 \operatorname{erfc}^{-1}(|\mathcal{S}|/m)$.

Substituting the last inequality into (58) and under our working assumption $|\mathcal{S}|/m \leq 0.25$, one readily obtains that

$$\|\mathbf{Bx}\|^2 \geq [1.4 \operatorname{erfc}^{-1}(|\mathcal{S}|/m)]^\gamma \cdot 0.99 |\mathcal{S}| [1 + \log(m/|\mathcal{S}|)] \geq 0.99 \cdot 1.14^\gamma |\mathcal{S}| [1 + \log(m/|\mathcal{S}|)] \quad (66)$$

which holds with probability exceeding $1 - e^{-c_2 m}$ for some absolute constant $c_2 > 0$, concluding the proof of Lemma 3.

D. Proof of Proposition 3

To proceed, let us introduce the following events for all $1 \leq i \leq m$:

$$\mathcal{D}_i := \left\{ (\mathbf{a}_i^* \mathbf{x})(\mathbf{a}_i^* \mathbf{z}) < 0 \right\} \quad (67)$$

$$\mathcal{E}_i := \left\{ \frac{|\mathbf{a}_i^* \mathbf{z}|}{|\mathbf{a}_i^* \mathbf{x}|} \geq \frac{1}{1+\eta} \right\} \quad (68)$$

for some fixed constant $\eta > 0$, in which the former corresponds to the gradients involving wrongly estimated signs, namely, $\frac{\mathbf{a}_i^* \mathbf{z}}{|\mathbf{a}_i^* \mathbf{z}|} \neq \frac{\mathbf{a}_i^* \mathbf{x}}{|\mathbf{a}_i^* \mathbf{x}|}$, and the second will be useful for deriving error bounds. Based on the definition of \mathcal{D}_i and with $\mathbb{1}_{\mathcal{D}_i}$ denoting the indicator function of the event \mathcal{D}_i , we have

$$\begin{aligned} \langle \ell_{\text{rw}}(\mathbf{z}), \mathbf{h} \rangle &= \frac{1}{m} \sum_{i=1}^m w_i \left(\mathbf{a}_i^* \mathbf{z} - |\mathbf{a}_i^* \mathbf{x}| \frac{\mathbf{a}_i^* \mathbf{z}}{|\mathbf{a}_i^* \mathbf{z}|} \right) (\mathbf{a}_i^* \mathbf{h}) \\ &= \frac{1}{m} \sum_{i=1}^m w_i \left(\mathbf{a}_i^* \mathbf{h} + \mathbf{a}_i^* \mathbf{x} - |\mathbf{a}_i^* \mathbf{x}| \frac{\mathbf{a}_i^* \mathbf{z}}{|\mathbf{a}_i^* \mathbf{z}|} \right) (\mathbf{a}_i^* \mathbf{h}) \\ &= \frac{1}{m} \sum_{i=1}^m w_i (\mathbf{a}_i^* \mathbf{h})^2 + \frac{1}{m} \sum_{i=1}^m 2w_i (\mathbf{a}_i^* \mathbf{x})(\mathbf{a}_i^* \mathbf{h}) \mathbb{1}_{\mathcal{D}_i} \end{aligned}$$

$$\geq \frac{1}{m} \sum_{i=1}^m w_i (\mathbf{a}_i^* \mathbf{h})^2 - \frac{1}{m} \sum_{i=1}^m 2w_i |\mathbf{a}_i^* \mathbf{x}| |\mathbf{a}_i^* \mathbf{h}| \mathbb{1}_{\mathcal{D}_i}. \quad (69)$$

In the following, we will derive a lower bound for the term on the right hand side of (69). To be specific, a lower bound for the first term $\frac{1}{m} \sum_{i=1}^m w_i (\mathbf{a}_i^* \mathbf{h})^2$ and an upper bound for the second term $\frac{1}{m} \sum_{i=1}^m 2w_i |\mathbf{a}_i^* \mathbf{x}| |\mathbf{a}_i^* \mathbf{h}| \mathbb{1}_{\mathcal{D}_i}$ will be obtained, which occupies Lemmas 5 and 6, with their proofs postponed to Appendix E and Appendix F, respectively.

Lemma 5. *Fix any $\eta, \beta > 0$. For any sufficiently small constant $\epsilon > 0$, the following holds with probability at least $1 - 2e^{-c_5 \epsilon^2 m}$:*

$$\frac{1}{m} \sum_{i=1}^m w_i (\mathbf{a}_i^* \mathbf{h})^2 \geq \frac{1 - \zeta_1 - \epsilon}{1 + \beta(1 + \eta)} \|\mathbf{h}\|^2 \quad (70)$$

with $w_i = \frac{1}{1 + \beta / (|\mathbf{a}_i^* \mathbf{z}| / |\mathbf{a}_i^* \mathbf{x}|)}$ for all $1 \leq i \leq m$, provided that $m/n > (c_6 \cdot \epsilon^{-2} \log \epsilon^{-1})$ for certain numerical constants $c_5, c_6 > 0$.

Now we turn to the second term in (69). For ease of exposition, let us first introduce the following events

$$\mathcal{B}_i := \{|\mathbf{a}_i^* \mathbf{x}| < |\mathbf{a}_i^* \mathbf{h}| \leq (k+1)|\mathbf{a}_i^* \mathbf{x}|\} \quad (71)$$

$$\mathcal{O}_i := \{(k+1)|\mathbf{a}_i^* \mathbf{x}| < |\mathbf{a}_i^* \mathbf{h}|\} \quad (72)$$

for all $1 \leq i \leq m$ and some fixed constant $k > 0$. The second term can be bounded as follows

$$\begin{aligned} \frac{1}{m} \sum_{i=1}^m 2w_i |\mathbf{a}_i^* \mathbf{x}| |\mathbf{a}_i^* \mathbf{h}| \mathbb{1}_{\mathcal{D}_i} &\leq \frac{1}{m} \sum_{i=1}^m w_i [(\mathbf{a}_i^* \mathbf{x})^2 + (\mathbf{a}_i^* \mathbf{h})^2] \mathbb{1}_{\{(\mathbf{a}_i^* \mathbf{z})(\mathbf{a}_i^* \mathbf{x}) < 0\}} \\ &= \frac{1}{m} \sum_{i=1}^m w_i [(\mathbf{a}_i^* \mathbf{x})^2 + (\mathbf{a}_i^* \mathbf{h})^2] \mathbb{1}_{\{(\mathbf{a}_i^* \mathbf{h})(\mathbf{a}_i^* \mathbf{x}) + (\mathbf{a}_i^* \mathbf{x})^2 < 0\}} \\ &\leq \frac{1}{m} \sum_{i=1}^m w_i [(\mathbf{a}_i^* \mathbf{x})^2 + (\mathbf{a}_i^* \mathbf{h})^2] \mathbb{1}_{\{|\mathbf{a}_i^* \mathbf{x}| < |\mathbf{a}_i^* \mathbf{h}|\}} \\ &\leq \frac{2}{m} \sum_{i=1}^m w_i (\mathbf{a}_i^* \mathbf{h})^2 \mathbb{1}_{\{|\mathbf{a}_i^* \mathbf{x}| < |\mathbf{a}_i^* \mathbf{h}|\}} \\ &= \frac{2}{m} \sum_{i=1}^m w_i (\mathbf{a}_i^* \mathbf{h})^2 \mathbb{1}_{\{|\mathbf{a}_i^* \mathbf{x}| < |\mathbf{a}_i^* \mathbf{h}| \leq (k+1)|\mathbf{a}_i^* \mathbf{x}|\}} \\ &\quad + \frac{2}{m} \sum_{i=1}^m w_i (\mathbf{a}_i^* \mathbf{h})^2 \mathbb{1}_{\{(k+1)|\mathbf{a}_i^* \mathbf{x}| < |\mathbf{a}_i^* \mathbf{h}|\}} \\ &= \frac{2}{m} \sum_{i=1}^m w_i (\mathbf{a}_i^* \mathbf{h})^2 \mathbb{1}_{\mathcal{B}_i} + \frac{2}{m} \sum_{i=1}^m w_i (\mathbf{a}_i^* \mathbf{h})^2 \mathbb{1}_{\mathcal{O}_i} \end{aligned} \quad (73)$$

where the first equality is derived by substituting $\mathbf{z} = \mathbf{h} + \mathbf{x}$ according to the definition of \mathbf{h} , the second event suffices for $(\mathbf{a}_i^* \mathbf{h})(\mathbf{a}_i^* \mathbf{x}) + (\mathbf{a}_i^* \mathbf{x})^2 < 0$, and the second equality follows from writing the indicator function $\mathbb{1}_{\{|\mathbf{a}_i^* \mathbf{x}| < |\mathbf{a}_i^* \mathbf{h}|\}}$ as the summation of two indicator functions of two events $\mathbb{1}_{\{|\mathbf{a}_i^* \mathbf{x}| < |\mathbf{a}_i^* \mathbf{h}| \leq (k+1)|\mathbf{a}_i^* \mathbf{x}|\}}$ and $\mathbb{1}_{\{|\mathbf{a}_i^* \mathbf{h}| > (k+1)|\mathbf{a}_i^* \mathbf{x}|\}}$.

The task so far remains to derive upper bounds for the two terms on the right side of (73), which leads to Lemma 6.

Lemma 6. Fixing some $k > 0$, define ζ_2 to be the maximum of $\mathbb{E}[w_i]$ in (82) for $\varrho = 0.01$ and $\nu = 0.1$, which depends only on k . For any $\epsilon > 0$, if $m/n > c_6 \epsilon^{-2} \log \epsilon^{-1}$, the following hold simultaneously with probability at least $1 - c_3 e^{-c_2 \epsilon^2 m}$:

$$\frac{1}{m} \sum_{i=1}^m w_i (\mathbf{a}_i^* \mathbf{h})^2 \mathbb{1}_{\mathcal{O}_i} \leq (\zeta_2 + \epsilon) \|\mathbf{h}\|^2 \quad (74)$$

and

$$\frac{1}{m} \sum_{i=1}^m w_i (\mathbf{a}_i^* \mathbf{h})^2 \mathbb{1}_{\mathcal{B}_i} \leq \frac{0.1271 - \zeta_2 + \epsilon}{1 + \beta/k} \|\mathbf{h}\|^2 \quad (75)$$

for all $\mathbf{h} \in \mathbb{R}^n$ obeying $\|\mathbf{h}\|/\|\mathbf{x}\| \leq 1/10$, where $c_1, c_2, c_3 > 0$ are some universal constants.

Taking the results in (70), (73), and (74)-(75) established in Lemmas 5 and 6 back into (69), we conclude that

$$\begin{aligned} \langle \ell_{\text{rw}}(\mathbf{z}), \mathbf{h} \rangle &\geq \frac{1}{m} \sum_{i=1}^m w_i (\mathbf{a}_i^* \mathbf{h})^2 \mathbb{1}_{\mathcal{E}_i} - \frac{1}{m} \sum_{i=1}^m 2w_i |\mathbf{a}_i^* \mathbf{x}| |\mathbf{a}_i^* \mathbf{h}| \mathbb{1}_{\mathcal{D}_i} \\ &\geq \frac{1 - \zeta_1 - \epsilon}{1 + \beta(1 + \eta)} \|\mathbf{h}\|^2 - 2(\zeta_2 + \epsilon) \|\mathbf{h}\|^2 - \frac{2(0.1271 - \zeta_2 + \epsilon)}{1 + \beta/k} \|\mathbf{h}\|^2 \\ &= \left[\frac{1 - \zeta_1 - \epsilon}{1 + \beta(1 + \eta)} - 2(\zeta_2 + \epsilon) - \frac{2(0.1271 - \zeta_2 + \epsilon)}{1 + \beta/k} \right] \|\mathbf{h}\|^2 \end{aligned} \quad (76)$$

which will be rendered positive, provided that $\beta > 0$ is small enough, and that parameters $\eta, k > 0$ are suitably chosen.

E. Proof of Lemma 5

Plugging in the weighting parameters $w_i = \frac{1}{1 + \beta / (|\mathbf{a}_i^* \mathbf{z}| / |\mathbf{a}_i^* \mathbf{x}|)}$ and based on the definition of \mathcal{E}_i , the first term in (69) can be lower bounded as follows

$$\frac{1}{m} \sum_{i=1}^m w_i (\mathbf{a}_i^* \mathbf{h})^2 \geq \frac{1}{m} \sum_{i=1}^m \frac{1}{1 + \beta / (|\mathbf{a}_i^* \mathbf{z}| / |\mathbf{a}_i^* \mathbf{x}|)} (\mathbf{a}_i^* \mathbf{h})^2 \mathbb{1}_{\mathcal{E}_i} \quad (77)$$

$$\begin{aligned} &\geq \frac{1}{m} \sum_{i=1}^m \frac{1}{1 + \beta(1 + \eta)} (\mathbf{a}_i^* \mathbf{h})^2 \mathbb{1}_{\left\{ \frac{|\mathbf{a}_i^* \mathbf{z}|}{|\mathbf{a}_i^* \mathbf{x}|} \geq \frac{1}{1 + \eta} \right\}} \\ &= \frac{1}{1 + \beta(1 + \eta)} \cdot \frac{1}{m} \sum_{i=1}^m (\mathbf{a}_i^* \mathbf{h})^2 \mathbb{1}_{\mathcal{E}_i} \end{aligned} \quad (78)$$

where the first inequality arises from dropping some nonnegative terms from the left hand side, and the second one replaced the ratio $|\mathbf{a}_i^* \mathbf{z}| / |\mathbf{a}_i^* \mathbf{x}|$ in the weights by its lower bound $1/(1+\eta)$ because the weights are monotonically increasing functions of the ratios $|\mathbf{a}_i^* \mathbf{z}| / |\mathbf{a}_i^* \mathbf{x}|$. Using the result in Lemma 7, the last term in (78) can be further bounded by

$$\frac{1}{m} \sum_{i=1}^m w_i (\mathbf{a}_i^* \mathbf{h})^2 \geq \frac{1}{1 + \beta(1 + \eta)} \cdot \frac{1}{m} \sum_{i=1}^m (\mathbf{a}_i^* \mathbf{h})^2 \mathbb{1}_{\mathcal{E}_i} \geq \frac{1 - \zeta_1 - \epsilon}{1 + \beta(1 + \eta)} \|\mathbf{h}\|^2 \quad (79)$$

for any fixed sufficiently small constant $\epsilon > 0$, which holds with probability at least $1 - 2e^{-c_5 \epsilon^2 m}$, if $m > (c_6 \cdot \epsilon^{-2} \log \epsilon^{-1})n$.

F. Proof of Lemma 6

The proof is adapted from that of [40, Lemma 9]. We first prove the bound (74) for any fixed \mathbf{h} obeying $\|\mathbf{h}\| \leq \|\mathbf{x}\|/10$, and subsequently develop a uniform bound at the end of this section. The bound (75) can be derived directly from subtracting the bound in (74) with k from that bound with $k = 0$, followed by an application of the Bernstein-type sub-exponential tail bound [32]. Hence, we only discuss the first bound (74). Because of the discontinuity hence non-Lipschitz of the indicator functions, let us approximate them by a sequence of auxiliary Lipschitz functions. Specifically, with some constant $\varrho > 0$, define for all $1 \leq i \leq m$ the ensuing continuous functions

$$\chi_i(s) := \begin{cases} s, & s > (1+k)^2(\mathbf{a}_i^* \mathbf{x})^2 \\ \frac{1}{\varrho}[s - (k+1)^2(\mathbf{a}_i^* \mathbf{x})^2] & (1-\varrho)(k+1)^2(\mathbf{a}_i^* \mathbf{x})^2 \leq s \leq (k+1)^2(\mathbf{a}_i^* \mathbf{x})^2 \\ 0, & \text{otherwise.} \end{cases} \quad (80)$$

Clearly, all $\chi_i(s)$'s are random Lipschitz functions with constant $1/\varrho$. Furthermore, it is easy to verify that

$$|\mathbf{a}_i^* \mathbf{h}|^2 \mathbb{1}_{\{(k+1)|\mathbf{a}_i^* \mathbf{x}| < |\mathbf{a}_i^* \mathbf{h}|\}} \leq \chi_i(|\mathbf{a}_i^* \mathbf{h}|^2) \leq |\mathbf{a}_i^* \mathbf{h}|^2 \mathbb{1}_{\{\sqrt{1-\varrho}(k+1)|\mathbf{a}_i^* \mathbf{x}| < |\mathbf{a}_i^* \mathbf{h}|\}}. \quad (81)$$

Given that the second term involves the addition event \mathcal{G}_i in (68), define $w_i := \frac{|\mathbf{a}_i^* \mathbf{h}|^2}{\|\mathbf{h}\|^2} \mathbb{1}_{\{\sqrt{1-\varrho}(k+1)|\mathbf{a}_i^* \mathbf{x}| < |\mathbf{a}_i^* \mathbf{h}|\}}$ for $1 \leq i \leq m$, and also $\nu := \frac{\|\mathbf{h}\|}{\|\mathbf{x}\|}$ for notational convenience. If $f(\tau_1, \tau_2)$ denotes the density of two joint Gaussian random variables with correlation constant $\rho = \frac{\mathbf{h}^* \mathbf{x}}{\|\mathbf{h}\| \|\mathbf{x}\|} \in (-1, 1)$, then the expectation of w_i can be obtained based on the conditional expectation

$$\begin{aligned} \mathbb{E}[w_i] &= \int_{-\infty}^{\infty} \mathbb{E}[w_i | \mathbf{a}_i^* \mathbf{x} = \tau_1 \|\mathbf{x}\|, \mathbf{a}_i^* \mathbf{h} = \tau_1 \|\mathbf{h}\|] f(\tau_1, \tau_2) d\tau_1 d\tau_2 \\ &= \int_{-\infty}^{\infty} \int_{-\infty}^{\infty} \tau_2^2 \mathbb{1}_{\{\sqrt{1-\varrho}(k+1)|\tau_1| < |\tau_2| \nu\}} f(\tau_1, \tau_2) d\tau_1 d\tau_2 \\ &= \frac{1}{\sqrt{2\pi}} \int_0^{\infty} \tau_2^2 \exp(-\tau_2^2/2) \left[\operatorname{erf} \left(\frac{(\nu/\sqrt{1-\varrho}(k+1)) - \rho \tau_2}{\sqrt{2(1-\rho^2)}} \right) \right. \\ &\quad \left. + \operatorname{erf} \left(\frac{(\nu/\sqrt{1-\varrho}(k+1)) + \rho \tau_2}{\sqrt{2(1-\rho^2)}} \right) \right] d\tau_2 \end{aligned} \quad (82)$$

$$:= \zeta_2. \quad (83)$$

It is not difficult to see that $\mathbb{E}[w_i] = 0$ for $\rho = \pm 1$, and $\mathbb{E}[w_i]$ is continuous over $\rho \in (-1, 1)$ due to the integration property of continuous functions over a continuous interval. Although the last term in (82) can not be expressed in closed-form, it can be evaluated numerically. Note first that for fixed parameters $\varrho > 0$ and $\nu \leq 0.1$, the integration above is monotonically decreasing in $k \geq 0$, and achieves the maximum at $k = 0$. For parameter values $k = 5$, $\nu = 0.1$ and $\varrho = 0.01$, Fig. 5 plots $\mathbb{E}[w_i]$ as a function of ρ , whose maximum $\zeta_2 = 0.0213$ is achieved at $\rho = 0$. Further from the integration in (82), for fixed $k \geq 0$, $\mathbb{E}[w_i]$ is a monotonically increasing function of both ν and ϱ , it is therefore safe to conclude that for all $0 < \nu \leq 0.1$, and $\varrho = 0.01$, we have

$$\mathbb{E}[w_i] \leq \zeta_2 = 0.0213. \quad (84)$$

Hence, it is safe to conclude that $\mathbb{E}[\chi_i(|\mathbf{a}_i^* \mathbf{h}|^2)] \leq 0.0213\|\mathbf{h}\|^2$ for $\nu < 0.1$, $\varrho = 0.01$, and $k = 5$. Since $\chi_i(|\mathbf{a}_i^* \mathbf{h}|^2)$'s are sub-exponential with sub-exponential norm of the order $\mathcal{O}(\|\mathbf{h}\|^2)$, Bernstein-type sub-exponential tail bound [32] confirms that

$$\mathbb{P}\left(\frac{1}{m} \sum_{i=1}^m \frac{\chi_i(|\mathbf{a}_i^* \mathbf{h}|^2)}{\|\mathbf{h}\|^2} > (\zeta_2 + \epsilon)\right) < e^{-c_7 m \epsilon^2} \quad (85)$$

for some numerical constant $\epsilon > 0$, provided that $\|\mathbf{h}\| \leq \|\mathbf{x}\|/10$. Finally, due to the fact that $w_i \leq 1$ for all $1 \leq i \leq m$, the following holds

$$\frac{1}{m} \sum_{i=1}^m w_i \chi_i(|\mathbf{a}_i^* \mathbf{h}|^2) < (\zeta_2 + \epsilon) \|\mathbf{h}\|^2 \quad (86)$$

with probability at least $1 - e^{-c_7 m \epsilon^2}$.

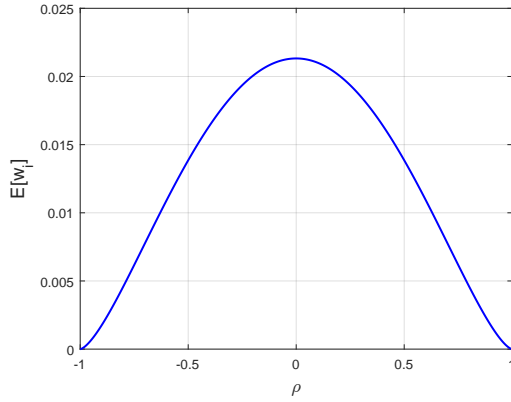


Fig. 5. The expectation $\mathbb{E}[w_i]$ as a function of ρ over $[-1, 1]$.

We have proved the bound in (74) for a fixed vector \mathbf{h} , and the uniform bound for all vectors \mathbf{h} obeying $\|\mathbf{h}\| \leq \|\mathbf{x}\|/10$ can be obtained by similar arguments in the proof [40, Lemma 9] with only minor changes in the constants.

Regarding the second bound (75), it is easy to see that

$$\begin{aligned} \frac{1}{m} \sum_{i=1}^m |\mathbf{a}_i^* \mathbf{h}|^2 \mathbb{1}_{\{|\mathbf{a}_i^* \mathbf{x}| < |\mathbf{a}_i^* \mathbf{h}| \leq (k+1)|\mathbf{a}_i^* \mathbf{x}|\}} &= \frac{1}{m} \sum_{i=1}^m |\mathbf{a}_i^* \mathbf{h}|^2 \mathbb{1}_{\{|\mathbf{a}_i^* \mathbf{x}| < |\mathbf{a}_i^* \mathbf{h}|\}} \\ &\quad - \frac{1}{m} \sum_{i=1}^m |\mathbf{a}_i^* \mathbf{h}|^2 \mathbb{1}_{\{(k+1)|\mathbf{a}_i^* \mathbf{x}| < |\mathbf{a}_i^* \mathbf{h}|\}} \\ &\leq (0.1271 - \zeta_2 + \epsilon) \|\mathbf{h}\|^2 \end{aligned} \quad (87)$$

where the last inequality follows from subtracting the bound in (74) of k from that corresponding to $k = 0$. To account for the weights $w_i = \frac{1}{1 + \beta/(|\mathbf{a}_i^* \mathbf{z}|/|\mathbf{a}_i^* \mathbf{x}|)}$, first notice that $\mathbf{a}_i^* \mathbf{h} = \mathbf{a}_i^* \mathbf{z} - \mathbf{a}_i^* \mathbf{x}$, and that our second bound works with $(\mathbf{a}_i^* \mathbf{z})(\mathbf{a}_i^* \mathbf{x}) < 0$ in (69), hence $\frac{|\mathbf{a}_i^* \mathbf{z}|}{|\mathbf{a}_i^* \mathbf{x}|} \leq \frac{|\mathbf{a}_i^* \mathbf{h}|}{|\mathbf{a}_i^* \mathbf{x}|} - 1$. Recall that the second bound (75)

assumes the event $\{|\mathbf{a}_i^* \mathbf{x}| < |\mathbf{a}_i^* \mathbf{h}| \leq (k+1)|\mathbf{a}_i^* \mathbf{x}|\}$, implying $\frac{|\mathbf{a}_i^* \mathbf{z}|}{|\mathbf{a}_i^* \mathbf{x}|} \leq \frac{|\mathbf{a}_i^* \mathbf{h}|}{|\mathbf{a}_i^* \mathbf{x}|} - 1 \leq k$. Further, because w_i is monotonically increasing in $\frac{|\mathbf{a}_i^* \mathbf{z}|}{|\mathbf{a}_i^* \mathbf{x}|}$, then $w_i \leq \frac{1}{1+\beta/k}$. Taking this result back to (87) yields

$$\frac{1}{m} \sum_{i=1}^m w_i |\mathbf{a}_i^* \mathbf{h}|^2 \mathbb{1}_{\{|\mathbf{a}_i^* \mathbf{x}| < |\mathbf{a}_i^* \mathbf{h}| \leq (k+1)|\mathbf{a}_i^* \mathbf{x}|\}} \leq \frac{0.1271 - \zeta_2 + \epsilon}{1 + \beta/k} \|\mathbf{h}\|^2 \quad (88)$$

which proves the second bound in (75).

Lemma 7. ([36, Lemma 5]) Fix $\eta \geq 1/2$ and $\rho \leq 1/10$, and let \mathcal{E}_i be defined in (67). For independent random variables $Y \sim \mathcal{N}(0, 1)$ and $Z \sim \mathcal{N}(0, 1)$, define

$$\zeta_1 := 1 - \min \left\{ \mathbb{E} \left[\mathbb{1}_{\left\{ \left| \frac{1-\rho}{\rho} + \frac{Y}{Z} \right| \geq \frac{\sqrt{1.01}}{\rho(1+\eta)} \right\}} \right], \mathbb{E} \left[Z^2 \mathbb{1}_{\left\{ \left| \frac{1-\rho}{\rho} + \frac{Y}{Z} \right| \geq \frac{\sqrt{1.01}}{\rho(1+\eta)} \right\}} \right] \right\}. \quad (89)$$

Fixing any $\epsilon > 0$ and for any \mathbf{h} satisfying $\|\mathbf{h}\|/\|\mathbf{x}\| \leq \rho$, the next holds with probability $1 - 2e^{-c_5 \epsilon^2 m}$:

$$\frac{1}{m} \sum_{i=1}^m (\mathbf{a}_i^* \mathbf{h})^2 \mathbb{1}_{\mathcal{E}_i} \geq (1 - \zeta_1 - \epsilon) \|\mathbf{h}\|^2 \quad (90)$$

provided that $m > (c_6 \cdot \epsilon^{-2} \log \epsilon^{-1})n$ for some universal constants $c_5, c_6 > 0$.

To have an estimate of the size of ζ_1 in (89), if $\gamma = 0.7$ and $\rho = 1/10$, we have $\mathbb{E} \left[\mathbb{1}_{\left\{ \left| \frac{1-\rho}{\rho} + \frac{Y}{Z} \right| \geq \frac{\sqrt{1.01}}{\rho(1+\gamma)} \right\}} \right] \approx 0.9216$, and $\mathbb{E} \left[Z^2 \mathbb{1}_{\left\{ \left| \frac{1-\rho}{\rho} + \frac{Y}{Z} \right| \geq \frac{\sqrt{1.01}}{\rho(1+\gamma)} \right\}} \right] \approx 0.9908$, hence leading to $\zeta_1 \approx 0.0784$.

REFERENCES

- [1] S. Bahmani and J. Romberg, "Phase retrieval meets statistical learning theory: A flexible convex relaxation," *arXiv:1610.04210*, 2016.
- [2] R. Balan, P. Casazza, and D. Edidin, "On signal reconstruction without phase," *Appl. Comput. Harmon. Anal.*, vol. 20, no. 3, pp. 345–356, May 2006.
- [3] A. S. Bandeira, J. Cahill, D. G. Mixon, and A. A. Nelson, "Saving phase: Injectivity and stability for phase retrieval," *Appl. Comput. Harmon. Anal.*, vol. 37, no. 1, pp. 106–125, 2014.
- [4] A. Ben-Tal and A. Nemirovski, *Lectures on Modern Convex Optimization: Analysis, Algorithms, and Engineering Applications*. SIAM, 2001, vol. 2.
- [5] T. Bendory and Y. C. Eldar, "Non-convex phase retrieval from STFT measurements," *arXiv:1607.08218*, 2016.
- [6] E. J. Candès and X. Li, "Solving quadratic equations via PhaseLift when there are about as many equations as unknowns," *Found. Comput. Math.*, vol. 14, no. 5, pp. 1017–1026, 2014.
- [7] E. J. Candès, X. Li, and M. Soltanolkotabi, "Phase retrieval via Wirtinger flow: Theory and algorithms," *IEEE Trans. Inf. Theory*, vol. 61, no. 4, pp. 1985–2007, Apr. 2015.
- [8] E. J. Candès, T. Strohmer, and V. Voroninski, "PhaseLift: Exact and stable signal recovery from magnitude measurements via convex programming," *Appl. Comput. Harmon. Anal.*, vol. 66, no. 8, pp. 1241–1274, Nov. 2013.
- [9] A. Chai, M. Moscoso, and G. Papanicolaou, "Array imaging using intensity-only measurements," *Inverse Probl.*, vol. 27, no. 1, p. 015005, Dec. 2011.
- [10] R. Chartrand and W. Yin, "Iteratively reweighted algorithms for compressive sensing," in *Proc. Intl. Conf. on Acoustics, Speech and Signal Process.*, Las Vegas, NV, USA, 2008, pp. 3869–3872.
- [11] J. Chen, L. Wang, X. Zhang, and Q. Gu, "Robust Wirtinger flow for phase retrieval with arbitrary corruption," *arXiv:1704.06256*, 2017.
- [12] P. Chen, A. Fannjiang, and G.-R. Liu, "Phase retrieval with one or two diffraction patterns by alternating projection with null initialization," *arXiv:1510.07379*, 2015.
- [13] Y. Chen, Y. Chi, and A. J. Goldsmith, "Exact and stable covariance estimation from quadratic sampling via convex programming," *IEEE Trans. Inf. Theory*, vol. 61, no. 7, pp. 4034–4059, Jul. 2015.

- [14] Y. Chen and E. J. Candès, “Solving random quadratic systems of equations is nearly as easy as solving linear systems,” *Comm. Pure Appl. Math.*, vol. 70, no. 5, pp. 822–883, Dec. 2017.
- [15] F. H. Clarke, “Generalized gradients and applications,” *T. Am. Math. Soc.*, vol. 205, pp. 247–262, 1975.
- [16] J. C. Duchi and F. Ruan, “Solving (most) of a set of quadratic equalities: Composite optimization for robust phase retrieval,” *arXiv:1705.02356*, 2017.
- [17] ———, “Stochastic methods for composite optimization problems,” *arXiv:1703.08570*, 2017.
- [18] Y. C. Eldar and S. Mendelson, “Phase retrieval: Stability and recovery guarantees,” *Appl. Comput. Harmon. Anal.*, vol. 36, no. 3, pp. 473–494, May 2014.
- [19] J. R. Fienup, “Phase retrieval algorithms: A comparison,” *Appl. Opt.*, vol. 21, no. 15, pp. 2758–2769, Aug. 1982.
- [20] R. W. Gerchberg and W. O. Saxton, “A practical algorithm for the determination of phase from image and diffraction,” *Optik*, vol. 35, pp. 237–246, Nov. 1972.
- [21] T. Goldstein and S. Studer, “PhaseMax: Convex phase retrieval via basis pursuit,” *arXiv:1610.07531v1*, 2016.
- [22] P. Hand and V. Voroninski, “An elementary proof of convex phase retrieval in the natural parameter space via the linear program PhaseMax,” *arXiv:1611.03935*, 2016.
- [23] R. H. Keshavan, A. Montanari, and S. Oh, “Matrix completion from a few entries,” *IEEE Trans. Inf. Theory*, vol. 56, no. 6, pp. 2980–2998, Jun. 2010.
- [24] R. Kueng, H. Rauhut, and U. Terstiege, “Low rank matrix recovery from rank one measurements,” *Appl. Comput. Harmon. Anal.*, vol. 42, no. 1, pp. 88–116, Jan. 2017.
- [25] Y. M. Lu and G. Li, “Phase transitions of spectral initialization for high-dimensional nonconvex estimation,” *arXiv:1702.06435*, 2017.
- [26] P. Netrapalli, P. Jain, and S. Sanghavi, “Phase retrieval using alternating minimization,” *IEEE Trans. Signal Process.*, vol. 63, no. 18, pp. 4814–4826, Sept. 2015.
- [27] J. R. Rice, *Numerical Methods in Software and Analysis*. Academic Press, 1992.
- [28] Y. Saad, *Numerical Methods for Large Eigenvalue Problems: Revised Edition*. SIAM, 2011.
- [29] Y. Shechtman, Y. C. Eldar, O. Cohen, H. N. Chapman, J. Miao, and M. Segev, “Phase retrieval with application to optical imaging: A contemporary overview,” *IEEE Signal Process. Mag.*, vol. 32, no. 3, pp. 87–109, May 2015.
- [30] M. Soltanolkotabi, “Structured signal recovery from quadratic measurements: Breaking sample complexity barriers via nonconvex optimization,” *arXiv:1702.06175*, 2017.
- [31] J. Sun, Q. Qu, and J. Wright, “A geometric analysis of phase retrieval,” *arXiv:1602.06664*, 2016.
- [32] R. Vershynin, “Introduction to the non-asymptotic analysis of random matrices,” *arXiv:1011.3027*, 2010.
- [33] I. Waldspurger, A. d’Aspremont, and S. Mallat, “Phase recovery, maxcut and complex semidefinite programming,” *Math. Program.*, vol. 149, no. 1, pp. 47–81, 2015.
- [34] G. Wang and G. B. Giannakis, “Solving random systems of quadratic equations via truncated generalized gradient flow,” in *Adv. Neural Inf. Process. Syst.*, Barcelona, Spain, 2016, pp. 568–576.
- [35] G. Wang, G. B. Giannakis, and J. Chen, “Scalable solvers of random quadratic equations via stochastic truncated amplitude flow,” *IEEE Trans. Signal Process.*, vol. 65, no. 8, pp. 1961–1974, Apr. 2017.
- [36] G. Wang, G. B. Giannakis, and Y. C. Eldar, “Solving systems of random quadratic equations via truncated amplitude flow,” *arXiv:1605.08285*, 2016.
- [37] G. Wang, L. Zhang, G. B. Giannakis, J. Chen, and M. Akçakaya, “Sparse phase retrieval via truncated amplitude flow,” *arXiv:1611.07641*, 2016.
- [38] X. Yi, C. Caramanis, and S. Sanghavi, “Alternating minimization for mixed linear regression,” in *Proc. Intl. Conf. on Mach. Learn.*, Beijing, China, 2014, pp. 613–621.
- [39] H. Zhang, Y. Chi, and Y. Liang, “Provable non-convex phase retrieval with outliers: Median truncated Wirtinger flow,” *arXiv:1603.03805*, 2016.
- [40] H. Zhang, Y. Zhou, Y. Liang, and Y. Chi, “Reshaped Wirtinger flow and incremental algorithm for solving quadratic system of equations,” *arXiv:1605.07719*, 2016.